

No. 2036

**TECHNICAL REPORT**

AD 641 888

MEASURED VERSUS COMPUTED  
SURFACE WAVE TRAINS  
OF A RANKINE OVOID

by

A. V. HERSHEY  
Computation and Analysis Laboratory

CLEARINGHOUSE FOR FEDERAL SCIENTIFIC AND TECHNICAL INFORMATION		
Hardcopy	Microfiche	
\$	\$	75 pp. 20
/ ARCHIVE COPY		



NOV 17 1966  
A

**U. S. NAVAL WEAPONS LABORATORY  
DAHLGREN, VIRGINIA**

U. S. Naval Weapons Laboratory  
Dahlgren, Virginia

MEASURED VERSUS COMPUTED

SURFACE WAVE TRAINS

OF A RANKINE OVOID

by

A. V. HERSHEY  
Computation and Analysis Laboratory

NWL REPORT NO. 2036

Task Assignment  
NO. R36OFR103/2101/R0110101

7 June 1966

Distribution of this document is unlimited.
--

## TABLE OF CONTENTS

	<u>Page</u>
Abstract . . . . .	ii
Foreword . . . . .	iv
Introduction . . . . .	1
Steady State . . . . .	5
Sourcewise Representation . . . . .	8
Free Surface . . . . .	10
Capillarity . . . . .	12
Transient State . . . . .	13
Surface Elevation . . . . .	23
Discussion . . . . .	24
Conclusion . . . . .	27
References . . . . .	28
Appendices:	
A. Schematic Diagram	
B. Tables I to V	
C. Figures 1 to 28	
D. Distribution	

### ABSTRACT

Measured elevations in the wave train of a Rankine ovoid are compared with computed elevations for an ideal source and sink. The measured elevations are in phase with the computed elevations but have smaller amplitudes. The discrepancy in amplitude is attributed to turbulent boundary layer and wake in the flow around the real ovoid.

### ZUSAMMENFASSUNG

Die gemessenen Höhen im Wellenzug eines Rankineschen eiförmigen Körpers werden mit den berechneten Höhen für eine ideale Quelle und Senke verglichen. Die gemessenen Höhen sind gleichphasig mit den berechneten, haben aber kleinere Amplituden. Die Unstimmigkeit hinsichtlich der Amplitude wird auf die turbulente Grenzschicht und die Nachlaufströmung am wahren eiförmigen Körper zurückgeführt.

### RESUME

On compare les élévations mesurées du train d'ondes d'un ovoïde de Rankine avec les élévations calculées pour une source et puits idéale. Les élévations mesurées sont en phase avec les élévations calculées, mais présentent des amplitudes plus réduites. La différence d'amplitude est attribuée à la couche limite et au sillage turbulents du courant qui entoure l'ovoïde réel.

## 摘要

ランキン卵形体より波列に於て測定された高さは理想涌き出しと吸い込みの計算された高さと比較される。測定高さは計算高さと同位相を有する、がその振幅は小さい。振幅の差は実卵形体のまわりの乱流境界層及び後流に帰する。

### FOREWORD

The material in this report was prepared as part of the foundational research program of the Naval Weapons Laboratory, Project NO. R360FR103, 2101/RO110101. Programming of machine computations on NORC was prepared by Mrs. E. J. Hershey. Analysis and computations were completed by 7 June 1966. The figures were prepared on a dot plotting cathode ray printer at the Naval Weapons Laboratory. The Japanese abstract and the schematic diagram were prepared on a vector plotting cathode ray printer at the David Taylor Model Basin.

APPROVED FOR RELEASE:

/s/ BERNARD SMITH  
Technical Director

## INTRODUCTION

A project at the Naval Weapons Laboratory has as its ultimate objective the computation of flow around surface ships of finite breadth in water of finite depth. In the pursuit of this project there has been prepared a system of four computing routines, which compute the components of velocity in the wave train of a point source.

A project at the David Taylor Model Basin has had as its objective the measurement of wave elevations in the wave train of a Rankine ovoid. When deeply submerged, the Rankine ovoid is that streamline of zero stream function which would be generated by a simple source and sink. A representative streamline is illustrated in Appendix A.

The wave elevations as measured at the David Taylor Model Basin present an ideal opportunity for a comparison with wave elevations as computed at the Naval Weapons Laboratory. One objective of the present report is to explore the possibility that the measured wave elevations might indicate how a sourcewise representation should be modified in order to allow for boundary layer and turbulent wake. Before any conclusions would be possible it has been necessary to evaluate in detail all sources of discrepancy between measured data and computed data.

The components of velocity in the wave train of a point source may be derived from the Havelock integral, which is a double Fourier integral in wave number space. The evaluation of the integral is achieved by radial and azimuthal integration in the wave number space. Following a suggestion from the David Taylor Model Basin, DiDonato<sup>1</sup> in 1958 developed a method of integration in which the path of integration is so displaced in the complex plane as to avoid a singularity in the integrand. Radial integration was performed by Simpson's rule and azimuthal integration was completed

with Gauss' rule. Without reference to this prior work, Yim<sup>2</sup> in 1963 has reexamined the problem of integration in the near field. With the aid of formulae of Barakat<sup>6</sup>, or after radial integration with Laguerre-Gauss quadrature, the azimuthal integration was completed with Legendre-Gauss quadrature. Yim examined also the problem of integration in the far field both along the center line behind the source and along the critical line of wave crests. However, the derivations were extended only as far as the first two terms of the asymptotic expansion in each case.

In the meantime, the present writer<sup>5</sup> has made an extensive investigation of possible methods of integration. At an early date it was realized that radial integration generates the complex exponential integral. In the sense that this function is an elementary function, the problem of integration is reduced to the problem of azimuthal integration alone. The high accuracy rule for the integration of a cyclical function is just the trapezoidal rule for equally spaced angles, and the above use of Gauss quadrature is not appropriate. Even the trapezoidal rule is inefficient for applications of importance to surface ships, and a new method of integration by parts was found in which integration could be performed through many oscillations of the integrand. It was recognized that the integrand is the product of a monotonic factor and an oscillatory factor. When the monotonic factor was approximated in terms of positive integral powers of the argument of the oscillatory factor, the integration could be completed by recourse to recurrence relations. Further improvement in efficiency was achieved through the expansion of the monotonic factor in terms of positive and negative half integral powers of the argument of the oscillatory factor. Finally the asymptotic series for stationary phase with quadratic approximation near the center line or with cubic approximation near the critical line has been carried to the ultimate term of smallest magnitude. These methods of integration are the basis for the four computing programs

for the computation of wave trains for a point source. The four programs provide computations with maximum efficiency or with controlled accuracy and with no limitation as to direction or distance from the point source. The programs were first reported in 1965.

All of the above work is concerned with the steady state wave pattern. In the integration of the double Fourier integral the classical approach was to use the Cauchy principal value but this led to a train of waves in front of the source as well as behind the source. Inasmuch as wave trains in front of the source are unacceptable on the basis of physical observation, the singularity in the integrand was avoided through the introduction of an imaginary term which is the so-called frictional term but is in reality merely a mathematical device to compel the path of integration in the complex plane to pass on the correct side of the singularity. An alternative approach is to recognize that the integrand at the point of singularity satisfies identically both the boundary equation and the Laplace equation and can be added therefore in arbitrary amount. When it is added in the correct amount to eliminate waves in front of the source, the integrand becomes analytic and the path of integration can be varied. A more convincing determination of the term to be added would be derived from an analysis of the limit approached by the transient disturbance which arises when a point source is started from rest and moves with constant velocity thereafter. Starting with a formula of Maruo<sup>7</sup>, an analysis was made by Hsu<sup>8</sup> in 1965, who concluded that there was a transient system of circular waves which were centered at the starting point and a stationary train of waves which trailed halfway back from the source to the starting point. In view of the importance of the transient waves as a guide to the properties of the stationary waves, the formula of Hsu is rederived herewith and is transformed further to reveal the character of the wave train.

The analysis of transient waves has been used by Hsu and Yim<sup>4</sup> in 1966 to interpret the experimental data on the wave profiles of the Rankine ovoid. Only the wave profiles on or near the center line were considered for interpretation whereas the wave profiles farther away from the center line are more interesting although more unstable. The experimental wave profiles were shifted with respect to time so as to match the theoretical wave profiles at a point of zero elevation. It was concluded from a comparison of the matched profiles that the ideal wave theory predicts wave profiles for fully submerged bodies with sufficient accuracy for practical purposes. On the other hand, a systematic discrepancy in amplitude of the measured and computed wave profiles was noted and was thought to be the result of viscous effects.

A series of determinations of wave profile have been made by D. A. Shaffer<sup>9,10</sup> at the David Taylor Model Basin. A Rankine ovoid was towed at various speeds, and wave elevations were recorded on a Sanborn recorder for various distances off the line of travel. The position of the ovoid was determined from the angle of rotation of a drum around which the towing cable was wrapped. Contacts on the drum transmitted signals which were recorded on the Sanborn record. Correction was made for slippage of the cable on the drum. The model was provided with a projecting lug which tripped a switch of known position and recorded a step on the Sanborn record. With this calibration the zero point of time when the center of the ovoid was opposite each recording station could be computed and marked on the record.

The ovoid had a length of  $4\frac{1}{2}$  ft with a ratio of length to diameter of 7. It was towed by a cable of  $\frac{1}{8}$ " diameter at a submergence of  $1\frac{1}{2}$  ft in water with a depth of 20 ft. The depth of submergence was uncertain to  $\pm 1.5$ " because of sag in the cable.

The length of travel at constant velocity was 205 ft. In one series of runs the wave elevation was measured at 0 ft and at 22.75 ft to one side of the line of travel while in another series of runs the wave elevation was measured at 11.375 ft and at 34.125 ft away from the line of travel. The speeds of the ovoid were 6, 7.3, 9, and 10 (ft)/(sec).

The amplitude of wave elevation was observed to fluctuate with speed with a minimum near 4 (ft)/(sec) and with a maximum near 7.3 (ft)/(sec). The minimum was interpreted in terms of interference while the maximum was correlated with critical Froude number.

Some deviation from a steady state wave profile occurred downstream from the model because there had not been enough time for the waves to develop their full height and because there was interference from waves which had been reflected off the walls of the basin. The unsteady region could be recognized by comparisons between records for different distances of travel. The length of the fully developed wave train was reported to be half of the distance of travel.

#### STEADY STATE

Let a point source be moving at a depth  $h$  below the surface with a speed  $U$ . A point in the fluid is located at Cartesian coordinates  $x, y, z$  in a right handed coordinate system with origin at the surface over the source. The  $x$ -coordinate is the distance forward, the  $y$ -coordinate is the distance to the right, and the  $z$ -coordinate is the distance downward. The velocity in the fluid is expressed

as the negative gradient of a velocity potential  $\varphi$ . The computing routines give the Cartesian components  $u$ ,  $v$ ,  $w$  of velocity in accordance with the equations

$$u = - \frac{\partial \varphi}{\partial x} \quad v = - \frac{\partial \varphi}{\partial y} \quad w = - \frac{\partial \varphi}{\partial z} \quad (1)$$

The velocity potential is the sum of three potentials in accordance with the equation

$$\varphi = \varphi_1 + \varphi_2 + \varphi_3 \quad (2)$$

where  $\varphi_1$  is the potential of the source in an unbounded fluid,  $\varphi_2$  is the potential of an image source over the free surface, and  $\varphi_3$  is a Fourier integral. The potentials  $\varphi_1 + \varphi_2$  cancel at the free surface, while the potential  $\varphi_3$  is the sum of a monotonic term and an oscillatory term. The monotonic term is responsible for a solitary wave or Bernoulli hump over the source while the oscillatory term is responsible for a wave train or Kelvin wake behind the source. Limiting formulae for the wave elevation on the line directly astern of a unit source may be derived from the asymptotic expansion of the potentials. For deep submergence the elevation in the solitary wave tends to vary like

$$2 \frac{U}{g} \frac{x}{(x^2 + h^2)^{\frac{3}{2}}} \quad (3)$$

Far down stream the elevation in the wave train tends to vary like

$$4\kappa_0 \left| \frac{2\pi}{gx} \right|^{\frac{1}{2}} e^{-\kappa_0 h} \cos(\kappa_0 x - \frac{\pi}{4}) \quad (4)$$

where the critical wave number  $\kappa_0$  is defined by the equation

$$\kappa_0 = \frac{g}{U^2} \quad (5)$$

The asymptotic formula for the wave train is not useful over the source where it goes to infinity.

It is of interest to note that when the source strength is proportional to  $U$  the amplitude in the wave train has a maximum with respect to  $U$  where

$$\kappa_0 h = \frac{1}{2} \quad (6)$$

This corresponds to a critical speed of 9.8 (ft)/(sec) when the depth of submergence is 1.5 ft.

The wave length  $\lambda$  of the waves directly behind the source is given by the equation

$$\lambda = \frac{2\pi}{\kappa_0} \quad (7)$$

Interference between a source and sink will occur if their distance apart is an integral multiple of wave length, while reinforcement will occur if their distance apart is half an odd integral multiple of wave length. Representative data for the experimental ovoid are given in the following table

Source Separation	Phase Correlation	Speed (ft)/(sec)
$\frac{3}{2}\lambda$	Reinforcement	3.7760
$\lambda$	Interference	4.6247
$\frac{1}{2}\lambda$	Reinforcement	6.5403

It may be noted that reinforcement prevails for the experimental speeds. Computed wave profiles have been obtained for the first two speeds in the above table together with the experimental speeds. The speeds, the critical wave numbers, and the wave lengths for which there are computed profiles are summarized in Table I.

### SOURCEWISE REPRESENTATION

The streamline for a deeply submerged source and sink was determined by iteration. Let the source and sink be of strength  $q$  at the positions  $\pm a$  on the  $x$ -axis. If the free stream velocity is unity, then the flux  $Q$  through any circle of radius  $r$  at the position  $x$  is given by the equation

$$Q = \pi r^2 - \frac{1}{2} \left\{ 1 - \frac{x - a}{\sqrt{(x - a)^2 + r^2}} \right\} q + \frac{1}{2} \left\{ 1 - \frac{x + a}{\sqrt{(x + a)^2 + r^2}} \right\} q \quad (8)$$

The equation of the streamline is  $Q = 0$ . In the limiting case where  $r \rightarrow 0$ , the equation of the streamline is reduced to

$$\frac{axq}{(x^2 - a^2)^2} = \pi \quad \left( x = \frac{l}{2} \right) \quad (9)$$

where  $x$  is the half length of the ovoid. In the limiting case where  $x \rightarrow 0$ , the equation of the streamline is reduced to

$$\frac{aq}{\sqrt{a^2 + r^2}} = \pi r^2 \quad \left( r = \frac{l}{14} \right) \quad (10)$$

where  $r$  is one seventh of the half length of the ovoid. Iterative solution of the simultaneous equations (9) and (10) for a length  $l = 4.5$  ft leads to the equations

$$a = 2.0884 \text{ ft} \quad q = 0.3284 (\text{ft})^2 \quad (11)$$

The radius  $r$  at any position  $x$  on the streamline is determined by the Newton-Raphson iteration

$$r \rightarrow r - \frac{Q}{\frac{\partial Q}{\partial r}} \quad (12)$$

In Table II are given recomputed values of radii for the same positions which were used in the specification of the model.<sup>8</sup> The recomputed values do not quite agree with the original values, but the discrepancies between values are not much more than a hundredth of an inch in the worst cases.

The partial derivatives of  $Q$  are given by the equations

$$\frac{\partial Q}{\partial x} = \frac{\frac{1}{2}r^2q}{\{(x-a)^2 + r^2\}^{\frac{3}{2}}} - \frac{\frac{1}{2}r^2q}{\{(x+a)^2 + r^2\}^{\frac{3}{2}}} \quad (13)$$

and

$$\frac{\partial Q}{\partial r} = 2\pi r - \frac{\frac{1}{2}r(x-a)q}{\{(x-a)^2 + r^2\}^{\frac{3}{2}}} + \frac{\frac{1}{2}r(x+a)q}{\{(x+a)^2 + r^2\}^{\frac{3}{2}}} \quad (14)$$

The components of unit vectors tangent or normal to the streamline can be expressed in terms of the partial derivatives of  $Q$ . Along a vertical plane of symmetry, the velocity normal to the streamline at a point is given by the expression

$$\frac{\frac{\partial Q}{\partial x}}{\sqrt{\left(\frac{\partial Q}{\partial x}\right)^2 + \left(\frac{\partial Q}{\partial r}\right)^2}}(u - v) \pm \frac{\frac{\partial Q}{\partial r}}{\sqrt{\left(\frac{\partial Q}{\partial x}\right)^2 + \left(\frac{\partial Q}{\partial r}\right)^2}}w \quad (15)$$

where the  $\pm$  sign depends upon whether the point is topside or bottomside. The sum of normal components of velocity for the source and sink is zero for deep submergence, but when the ovoid is near the surface, there are contributions to velocity from the surface waves. The resultant velocity for the source and sink does not quite give a vanishing normal component at the surface of the ovoid. The normal component at the vertical plane has been computed for the experimental conditions. The worst case was for 6 (ft)/(sec) where the normal component was not more than 1.6% of the free stream velocity.

### FREE SURFACE

One of the errors in the mathematical model is a linearization of the boundary condition at the free surface. Let the equation of the free surface be

$$z - f(x, y) = 0 \quad (16)$$

For steady state conditions the velocity potential at the free surface satisfies the boundary equation

$$\left( U + \frac{\partial \varphi}{\partial x} \right) \frac{\partial f}{\partial x} + \frac{\partial \varphi}{\partial y} \frac{\partial f}{\partial y} - \frac{\partial \varphi}{\partial z} = 0 \quad (17)$$

and also the Bernoulli equation

$$\frac{1}{2} \left\{ \left( U + \frac{\partial \varphi}{\partial x} \right)^2 + \left( \frac{\partial \varphi}{\partial y} \right)^2 + \left( \frac{\partial \varphi}{\partial z} \right)^2 \right\} - gf = \frac{1}{2} U^2 \quad (18)$$

which becomes the equation

$$U \frac{\partial^2 \varphi}{\partial x^2} + \frac{1}{2} \frac{\partial}{\partial x} \left\{ \left( \frac{\partial \varphi}{\partial x} \right)^2 + \left( \frac{\partial \varphi}{\partial y} \right)^2 + \left( \frac{\partial \varphi}{\partial z} \right)^2 \right\} - g \frac{\partial f}{\partial x} = 0 \quad (19)$$

after differentiation with respect to  $x$ . To the first order of small quantities the equation of the surface is

$$f = \frac{U}{g} \frac{\partial \varphi}{\partial x} \quad (20)$$

whence the derivatives of  $f$  are given by the equations

$$\frac{\partial f}{\partial x} = \frac{U}{g} \frac{\partial^2 \varphi}{\partial x^2} \qquad \frac{\partial f}{\partial y} = \frac{U}{g} \frac{\partial^2 \varphi}{\partial x \partial y} \qquad (21)$$

Substitution of these expressions of first order into the expressions of second order leads to the second order boundary equation

$$\frac{\partial^2 \varphi}{\partial x^2} - \kappa_0 \frac{\partial \varphi}{\partial z} + \frac{1}{U} \frac{\partial}{\partial x} \left\{ \left( \frac{\partial \varphi}{\partial x} \right)^2 + \left( \frac{\partial \varphi}{\partial y} \right)^2 + \frac{1}{2} \left( \frac{\partial \varphi}{\partial z} \right)^2 \right\} = 0 \qquad (22)$$

The second order term in this equation is the derivative of a quantity which is positive and fluctuates between minima and maxima such that the minima are about half the adjacent maxima in magnitude. The wave number of the fluctuation of the second order term is twice the wave number of the fluctuation of first order terms. The neglect of the second order term in the boundary equation leads to an error in elevation whose amplitude is estimated to be equal to the maxima of the quantity

$$\frac{1}{g} \left\{ \left( \frac{\partial \varphi}{\partial x} \right)^2 + \left( \frac{\partial \varphi}{\partial y} \right)^2 + \frac{1}{2} \left( \frac{\partial \varphi}{\partial z} \right)^2 \right\} \qquad (23)$$

Values of this quantity have been computed for the experimental conditions and the largest maxima for each speed are summarized in Table III. The largest error in elevation is only about 2.0% of the largest amplitude of elevation.

### CAPILLARITY

Another error in the mathematical model arises from a neglect of surface tension at the free surface. A surface tension  $\gamma$  acts on a line element  $d\mathbf{r}$  in the surface in a direction which lies in the surface and is orthogonal to  $d\mathbf{r}$ . The component of this force in the direction of increasing  $z$  is given by the product of this force and the rate of change of  $f$  in the direction orthogonal to  $d\mathbf{r}$ . The component of force is given by the scalar product

$$- \gamma \nabla f \cdot \mathbf{k} \times d\mathbf{r} \quad (24)$$

where  $\mathbf{k}$  is a unit vector in the direction of increasing  $z$ . The resultant force on a closed contour with position vector  $\mathbf{r}$  is given by the circuit integral

$$- \gamma \oint \nabla f \cdot \mathbf{k} \times d\mathbf{r} \quad (25)$$

where the path of integration is taken in the right-handed direction relative to the vector  $\mathbf{k}$ . The surface tension on the contour is balanced by the action of a pressure against that surface which is contained within the contour. Application of triple product expansions and of the Stokes theorem to the circuit integral shows that the pressure is given by the equation

$$p = \gamma \nabla \cdot \nabla f \quad (26)$$

The Bernoulli equation is modified therefore through addition of the term

$$\frac{\gamma}{\rho} \left( \frac{\partial^2 f}{\partial x^2} + \frac{\partial^2 f}{\partial y^2} \right) \quad (27)$$

and to first order the boundary equation becomes

$$\frac{\partial^2 \varphi}{\partial x^2} - x_0 \frac{\partial \varphi}{\partial z} - \frac{\gamma}{\rho g} \frac{\partial^4 \varphi}{\partial x^2 \partial z^2} = 0 \quad (28)$$

The effect of surface tension is a change in amplitude and wave length by the fractional amount

$$\frac{\gamma}{\rho g} x_0^2 \quad (29)$$

Inasmuch as the coefficient of  $x_0^2$  in this expression is on the order of

$$\frac{\gamma}{\rho g} = 8 \times 10^{-5} \text{ (ft)}^2 \quad (30)$$

the effect of surface tension was negligible for the experimental conditions. The effect of capillarity is not important as long as the towing speed substantially exceeds the minimum speed<sup>12</sup> of 0.76 (ft)/(sec).

#### TRANSIENT STATE

The ovoid was started and stopped in a tank of finite size. Only a limited part of the recorded wave elevation approximates the limiting profile for steady state. The extent of good profile can be deduced from an analysis of the transient wave pattern.

Let the Cartesian coordinates  $x, y, z$  of a point in the fluid at time  $t$  be referred to a fixed origin with  $z$  measured downward.

Let the velocity in the fluid be the negative gradient  $-\nabla\varphi$  of a velocity potential  $\varphi$  which is a solution of Laplace's equation  $\nabla \cdot \nabla\varphi = 0$ . The dynamical equation is the Bernoulli equation

$$-\frac{\partial\varphi}{\partial t} + \frac{1}{2}(\nabla\varphi)^2 + \frac{p}{\rho} - gz = \text{constant} \quad (31)$$

where  $\rho$  is the density,  $p$  is the pressure, and  $g$  is the acceleration of gravity. Let the equation of the free surface be

$$z = f(x, y, t) \quad (32)$$

and let a source be created below the origin at a depth  $h$  and at the time zero in a fluid initially at rest.

In the limit of instantaneous formation of a finite source all terms in the Bernoulli equation including  $p/\rho$  remain bounded at the free surface and  $\partial\varphi/\partial t$  therefore must also remain bounded at the free surface. If each term in the Bernoulli equation is integrated with respect to time, then the term  $\partial\varphi/\partial t$  becomes the change in potential but the other terms become infinitesimals. In the limit of instantaneous formation of the source the potential remains constant, and the boundary conditions require that the formation of a source beneath the surface be accompanied by the formation of an image over the surface. For a unit source below the surface the potential  $\varphi_1$  is given by the equation

$$\varphi_1 = \frac{1}{\sqrt{x^2 + y^2 + (z - h)^2}} \quad (33)$$

and for an image source over the surface the potential  $\varphi_2$  is given by the equation

$$\varphi_2 = - \frac{1}{\sqrt{x^2 + y^2 + (z + h)^2}} \quad (34)$$

The Fourier transforms of the potentials  $\varphi_1$  and  $\varphi_2$  are given by the equations

$$\varphi_1 = \frac{1}{2\pi} \int_{-\pi}^{+\pi} \int_0^{\infty} e^{-x|z-h| + ix(x\cos\theta + y\sin\theta)} dx d\theta \quad (35)$$

and

$$\varphi_2 = - \frac{1}{2\pi} \int_{-\pi}^{+\pi} \int_0^{\infty} e^{-x(z+h) + ix(x\cos\theta + y\sin\theta)} dx d\theta \quad (36)$$

To these must be added a potential  $\varphi_3$  which is initially zero but meets the boundary conditions at the free surface.

The linearized Bernoulli equation at the free surface is

$$\frac{\partial \varphi}{\partial t} + gf = 0 \quad (37)$$

while the kinematic equation at the free surface is

$$\frac{\partial \varphi}{\partial z} + \frac{\partial f}{\partial t} = 0 \quad (38)$$

Elimination of  $f$  from Equations (37) and (38) leads to the boundary equation

$$\frac{\partial^2 \varphi}{\partial t^2} - g \frac{\partial \varphi}{\partial z} = 0 \quad (39)$$

The Fourier amplitude  $A(\kappa, \theta, t)$  of the potential  $\varphi$ , therefore satisfies the equation

$$\frac{\partial^2 A}{\partial t^2} + \kappa g A - \frac{g}{\pi} = 0 \quad (40)$$

of which the appropriate solution is

$$A(\kappa, \theta, t) = \frac{1}{\pi \kappa} - \frac{\cos \sqrt{g \kappa} t}{\pi \kappa} \quad (41)$$

If an instantaneous creation of a finite source is followed after a time interval  $dt$  by the instantaneous annihilation of the finite source, then the Fourier amplitude per unit pulse is merely

$$A(\kappa, \theta, t) = \frac{1}{\pi} \sqrt{\frac{g}{\kappa}} \sin \sqrt{g \kappa} t \quad (42)$$

and from the boundary equation (37) the surface elevation per unit pulse is given by the equation

$$-f = \frac{1}{\pi} \int_{-\pi}^{+\pi} \int_0^\infty \cos \sqrt{g \kappa} t e^{-\kappa z + i \kappa (x \cos \theta + y \sin \theta)} \kappa d\kappa d\theta \quad (43)$$

The surface elevation is initially a hump but breaks ultimately into the well known system of concentric waves.

An alternative formulation is achieved through the substitution

$$x \cos \theta + y \sin \theta = r \cos \phi \quad (44)$$

and from the definition<sup>13</sup>

$$J_0(z) = \frac{1}{\pi} \int_0^\pi \cos(z \cos \phi) d\phi \quad (45)$$

The surface elevation per unit pulse is given by the equation

$$-f = 2 \int_0^\infty \cos \sqrt{gk} t e^{-kh} J_0(kr) k dk \quad (46)$$

From the Lipschitz integral<sup>13</sup> the equation for the hump at  $t = 0$  is recovered. The initial surface elevation thus is given by the equation

$$-f = \frac{2h}{(h^2 + r^2)^{\frac{3}{2}}} \quad (t = 0) \quad (47)$$

After a number of complex transformations of variable the elevation for  $r = 0$  is obtained. The surface elevation at the origin is given by the equation

$$-f = \frac{2}{h^2} \left[ 1 - \frac{gt^2}{4h} - \left( \frac{3}{2} - \frac{gt^2}{4h} \right) \left( \frac{gt^2}{4h} \right)^{\frac{1}{2}} e^{-\frac{gt^2}{4h}} \int_0^{\frac{gt^2}{4h}} \frac{e^{-u}}{u^{\frac{3}{2}}} du \right] \quad (r = 0) \quad (48)$$

The integral in this equation is the Fresnel integral of imaginary argument. The surface elevation at the origin subsides gradually with time until it is negative, then becomes positive, and finally returns to zero.

If the Bessel function in Equation (46) is replaced by its asymptotic value,

$$J_0(\kappa r) = \left(\frac{2}{\pi \kappa r}\right)^{\frac{1}{2}} \cos\left(\kappa r - \frac{\pi}{4}\right) \quad (49)$$

then there appears in the integrand the product

$$\cos\left(\kappa r - \frac{\pi}{4}\right) \cos\sqrt{g\kappa} t \quad (50)$$

This product makes the most contribution to the integration when the arguments of its factors differ by a multiple  $n$  of  $2\pi$  and furthermore the derivatives of these arguments are equal. The product then behaves like the square of a cosine and is positive over the longest range of integration. The derivatives are equal when

$$r = \frac{1}{2} \sqrt{\frac{g}{\kappa}} t \quad (51)$$

and the arguments differ by a multiple of  $2\pi$  when

$$\frac{gt^2}{4r} = 2n\pi - \frac{\pi}{4} \quad (52)$$

The amplitude of the waves is limited by the exponential function in the integrand of Equation (46). Since neither the trigonometric function nor the Bessel function are ever more than unity, the amplitude cannot exceed the initial elevation at the origin.

If a unit source is created below the origin at depth  $h$  and at time zero and then moves along the  $x$ -axis at constant speed  $U$ , the elevation of the surface may be obtained through integration of the effects of pulses which have been created during a succession of differential time intervals  $d\tau$  from  $\tau = 0$  to  $\tau = t$ . The resultant elevation at time  $t$  thus is given by the equation

$$-f = \frac{1}{\pi} \iiint \cos \sqrt{gk} (t - \tau) e^{-kx + ik\{(x - U\tau)\cos\theta + y\sin\theta\}} k dx d\theta d\tau \quad (53)$$

Integration with respect to  $\tau$  leads to a formula equivalent to that of Hsu<sup>3</sup>, while further development in terms of half time leads to the equation

$$\begin{aligned} -f = & \frac{1}{\pi} \iint \frac{\sin \frac{1}{2}(\sqrt{gk} + kU \cos \theta)t}{\sqrt{gk} + kU \cos \theta} e^{-kx + ik\{(x - \frac{Ut}{2})\cos\theta + y\sin\theta\} + \frac{i}{2}\sqrt{gk}t} k dx d\theta \\ & + \frac{1}{\pi} \iint \frac{\sin \frac{1}{2}(\sqrt{gk} - kU \cos \theta)t}{\sqrt{gk} - kU \cos \theta} e^{-kx + ik\{(x - \frac{Ut}{2})\cos\theta + y\sin\theta\} - \frac{i}{2}\sqrt{gk}t} k dx d\theta \end{aligned} \quad (54)$$

In the limit as  $t \rightarrow \infty$  there is no major contribution to the integration except in the neighborhood of a singularity of the denominator of either integrand where

$$u \equiv k - \frac{k_0}{\cos^2 \theta} \sim 0 \quad (55)$$

Local expansions in terms of  $u$  in the neighborhood of a singularity are given by the equations

$$\sqrt{g}x \pm uU \cos \theta = -\frac{1}{2}U|\cos \theta|u + \dots \quad (56)$$

and

$$ix\{(x - \frac{1}{2}Ut)\cos \theta + y \sin \theta\} \pm \frac{i}{2}\sqrt{g}xt = \frac{ix_0}{\cos^2 \theta} \{(x - Ut)\cos \theta + y \sin \theta\} + i\{(x - \frac{3}{4}Ut)\cos \theta + y \sin \theta\}u + \dots \quad (57)$$

Required for the evaluation in the limit as  $t \rightarrow \infty$  is the remarkable integral

$$\int_0^\infty \frac{\sin au \cos bu}{u} du = \begin{cases} 0 & \text{if } |a| < |b| \\ \frac{\pi}{2} & \text{if } |a| > |b| \end{cases} \quad (58)$$

where  $a$  is positive but  $b$  may be of either sign and  $a, b$  are identified as follows:

$$a = \frac{1}{4}U|\cos \theta|t \quad b = (x - \frac{3}{4}Ut)\cos \theta + y \sin \theta \quad (59)$$

The nonzero part of the wave train is confined between boundaries where  $|a| \geq |b|$ .

The leading edge of the wave train is defined by the equation

$$(x - Ut)\cos \theta + y \sin \theta = 0 \quad (60)$$

and the trailing edge is defined by the equation

$$(x - \frac{1}{2}Ut)\cos\theta + y\sin\theta = 0 \quad (61)$$

Whether the boundary of the wave train is inclined forward or backward depends upon the signs of  $\sin\theta$  and  $\cos\theta$  at the points of stationary phase. The phase is stationary where

$$\frac{d}{d\theta} \left( \frac{x - Ut}{\cos\theta} + \frac{y\sin\theta}{\cos^2\theta} \right) = 0 \quad (62)$$

or where

$$y\sin\theta = - \frac{\sin^2\theta}{1 + \sin^2\theta} \cos\theta (x - Ut) \quad (63)$$

Substitutions from Equation (63) into Equations (60), (61) show that the wave train is confined to the region where  $x$  satisfies the inequality

$$\frac{1}{2}Ut \cos^2\theta < x < Ut \quad (64)$$

Along the center line where  $y = 0$  the trailing edge of the wave train is at  $x = \frac{1}{2}Ut$  while along the critical line of wave crests where

$\theta = \sin^{-1} \frac{1}{\sqrt{3}}$  the trailing edge is at  $x = \frac{1}{3}Ut$ . The divergent waves

extend farther back than the transverse waves, as might be expected from a simple Huygens construction.

When Equation (54) is so rearranged as to replace  $x - \frac{1}{2}Ut$  by  $x - Ut$  the result is the equation

$$\begin{aligned}
 -f = & \frac{1}{2\pi} \iint \frac{\sin(\sqrt{gk} + kU \cos \theta)t}{\sqrt{gk} + kU \cos \theta} e^{-kh + ik\{(x - Ut)\cos \theta + y \sin \theta\}} k dk d\theta \\
 & + \frac{1}{2\pi} \iint \frac{\sin(\sqrt{gk} - kU \cos \theta)t}{\sqrt{gk} - kU \cos \theta} e^{-kh + ik\{(x - Ut)\cos \theta + y \sin \theta\}} k dk d\theta \\
 & + \frac{i}{\pi} \iint \frac{\sin^{\frac{21}{2}}(\sqrt{gk} + kU \cos \theta)t}{\sqrt{gk} + kU \cos \theta} e^{-kh + ik\{(x - Ut)\cos \theta + y \sin \theta\}} k dk d\theta \\
 & - \frac{i}{\pi} \iint \frac{\sin^{\frac{21}{2}}(\sqrt{gk} - kU \cos \theta)t}{\sqrt{gk} - kU \cos \theta} e^{-kh + ik\{(x - Ut)\cos \theta + y \sin \theta\}} k dk d\theta \quad (65)
 \end{aligned}$$

In the first two integrals of this equation there is no major contribution to the integration except in the neighborhood of the singularity as before where a local expansion can be made in terms of  $u$ . The integration requires the value of the integral

$$\int_0^{\infty} \frac{\sin au}{u} du = \frac{\pi}{2} \quad (a > 0) \quad (66)$$

where  $a$  is defined now by the equation

$$a = \frac{1}{2}U|\cos \theta|t \quad (67)$$

In the second two integrals the integrands are multiplied by the square of a sine which is always positive and in the limit as  $t \rightarrow \infty$  has the effect of weighting the Cauchy principal value by  $\frac{1}{2}$ .

The first two integrals lead to the singular term which must be added to the steady state solution to eliminate waves ahead of the source while the second two integrals lead to the Cauchy principal value which gives waves ahead as well as behind the source.

#### SURFACE ELEVATION

The components of velocity for the steady state have been computed on NORC at 0.5221 ft intervals in  $x$  from 52.21 ft ahead of the line of wave crests to 104.42 ft behind the line of wave crests. The data for  $u$  at  $\pm 2.0684$  ft from the midpoint between sources were multiplied by the quantity

$$\frac{g}{4\pi\alpha_0} \quad (68)$$

and were subtracted to obtain the computed wave elevations for the simple source and sink. The data for  $x$  were converted to time through division by  $U$ . The computed wave elevations are plotted against time as solid lines in Figures 1 to 28.

In order to obtain digital values of the experimental results for comparison with the computed results, readings have been taken at 0.1 sec intervals from the Sanborn records in reference 10. The records for 153 ft of travel have been selected for utilization in the present analysis because the data for this distance of travel were understood to be the most reliable. Some discrepancies in zero point settings were noted and were called to the attention of Mr. Shaffer, who has reanalysed the data and has obtained more accurate results. The improved data are plotted as dotted lines in Figures 9 to 24.

The timing of the experimental data is believed to have a precision of  $\pm 0.02$  sec but some remaining inconsistency suggests that the accuracy may be less. Thus the agreement between theory and experiment is better for those runs where the distances off center line were 0 and  $22\frac{3}{4}$  ft than it is where the distances off center line were  $11\frac{3}{8}$  ft and  $34\frac{1}{4}$  ft. The discrepancy is especially evident in Figures 10, 14, and 22 where the experimental wave profiles lead the theoretical wave profiles.

### DISCUSSION

The theoretical and experimental wave profiles compare quite favorably with respect to phase in the range of fully developed wave train and there is correspondence between double wave crests at higher speed. There is some disagreement as to amplitude, however, part of which may arise from uncertainty as to depth of submergence. That this may have a substantial effect on amplitude is indicated by Table IV where the estimated decrease in amplitude for 1.5" increase in depth is listed. The effect decreases with increase in speed and is relatively unimportant at 10 (ft)/(sec). A checkrun for this speed with the depth increased from 1.5' to 1.625' confirmed the predicted decrease in amplitude and indicated that wave shape was not appreciably affected.

The tests were run in water of finite depth and at the highest speed the wave length of the transverse waves was nearly equal to the depth of water in the tank. A checkrun with a computing routine for finite depth showed that the effect was negligible even at 10 (ft)/(sec) speed.

The duration of good wave train is terminated when the trailing edge of the wave train passes the recording station. The elapsed time from the passage of the model to the passage of the trailing edge is the time for the trailing edge to advance the remaining

half distance at half of the speed of the model. Times of termination in seconds are given in Table V. These values are for the limiting case of infinite time and the actual durations of steady wave train tend to be less.

After the model has stopped the wave train tends to persist undiminished except at the tip which becomes rounded off. The rate of propagation of the tip of the wave train is reduced to group velocity or to half the model speed. The residual wave train is reflected from the far wall of the tank but should not perturb the recorded elevation until after the reflection has returned to the recording station. The reflecting wall of the tank was more than 271 ft from the starting point of the model, and the residual wave would not be reflected back to the recording station in less time than it would take the trailing edge of the wave train to reach the recording station. It must be concluded that the recorded data for 133 ft of travel offer a shorter duration of good wave train than the data for 187 ft of travel. Whereas the data for 133 ft of travel were used in the preparation of Figures 1 to 24, the data for 187 ft of travel have been used in the supplementary Figures 25 to 28. The better agreement between measured and computed elevations for the greater distance is noteworthy.

Error in the boundary conditions of the mathematical model cannot contribute more than a few per cent error to the amplitude of elevation. The assumption of ideal flow should be valid at the free surface which is several radii above the test model, but the assumption of a simple source and sink is undoubtedly in error because of boundary layer and wake. During the towing tests the Reynolds number of the model was in the range  $2 \times 10^6$  to  $4 \times 10^6$ . It seems likely that the flow over the model was fully turbulent, inasmuch as the model was preceded by a long towing cable which could induce turbulence at the nose of the model. The simplest effect of boundary layer separation with trailing flow in the wake would be a reduction in strength and a backward displacement of the

sink. The reduction in strength could be inferred from the drag on the ovoid but there do not seem to be data on drag for Rankine ovoids, and data on drag for torpedoes could not be extrapolated because of disparities in prismatic coefficient. The drag for a Rankine ovoid is probably at least as great as the drag for a sphere of the same diameter.

The presence of a boundary layer has the effect of slowing down the real flow with respect to the ideal flow with a spreading of the streamlines in the neighborhood. The spreading becomes pronounced toward the rear where there is separation of the boundary layer. The decrease of longitudinal flow in the turbulent wake is compensated by a decrease of convergent flow to the sink. The decrease of flow may be inferred from the drag or rate of transfer of momentum to the fluid. The drag  $D$  is given by the equation

$$D = \frac{1}{2} \rho U^2 S C_D = 2 \pi \rho U \int_0^{\infty} u r dr \quad (69)$$

where  $S$  is the projected area,  $C_D$  is the drag coefficient, and the integration of longitudinal speed  $u$  is with respect to distance  $r$  from the axis of the wake. For a sphere of diameter  $d$  the projected area is given by the equation

$$S = \frac{1}{4} \pi d^2 \quad (70)$$

while the fractional reduction in the flow is given by the equation

$$\frac{2 \pi \int_0^{\infty} u r dr}{\frac{1}{4} \pi d^2 U} = \frac{1}{2} C_D \quad (71)$$

At the experimental values of the Reynold's number the drag coefficient<sup>11</sup> is on the order of 0.2 for a sphere and the reduction of strength of the sink should be at least 10% for the ovoid. That it is closer to 25% can be inferred easily from reruns of the computations with the strength of the sink reduced by appropriate amounts. It is desirable that the matter be settled more definitely with the aid of photographic data as determined from smoke traces in air tunnels or from bubble traces in water tunnels.

Since the preparation of this report, a model of the Rankine ovoid has been made at the Naval Weapons Laboratory and is being tested at the Notre Dame University. Preliminary photographs<sup>14</sup> with smoke traces indicate a detectable spreading of the streamlines behind the ovoid. Improvements in experimental design will be necessary before quantitative conclusions can be drawn from the experimental streamlines.

### CONCLUSION

The experimental and theoretical wave profiles compare quite favorably in view of experimental difficulties. The principal error in the theoretical wave profiles arose from the use of a simple source and sink for an approximation of the ovoid. The sourcewise approximation could be improved from an analysis of experimental data on streamlines.

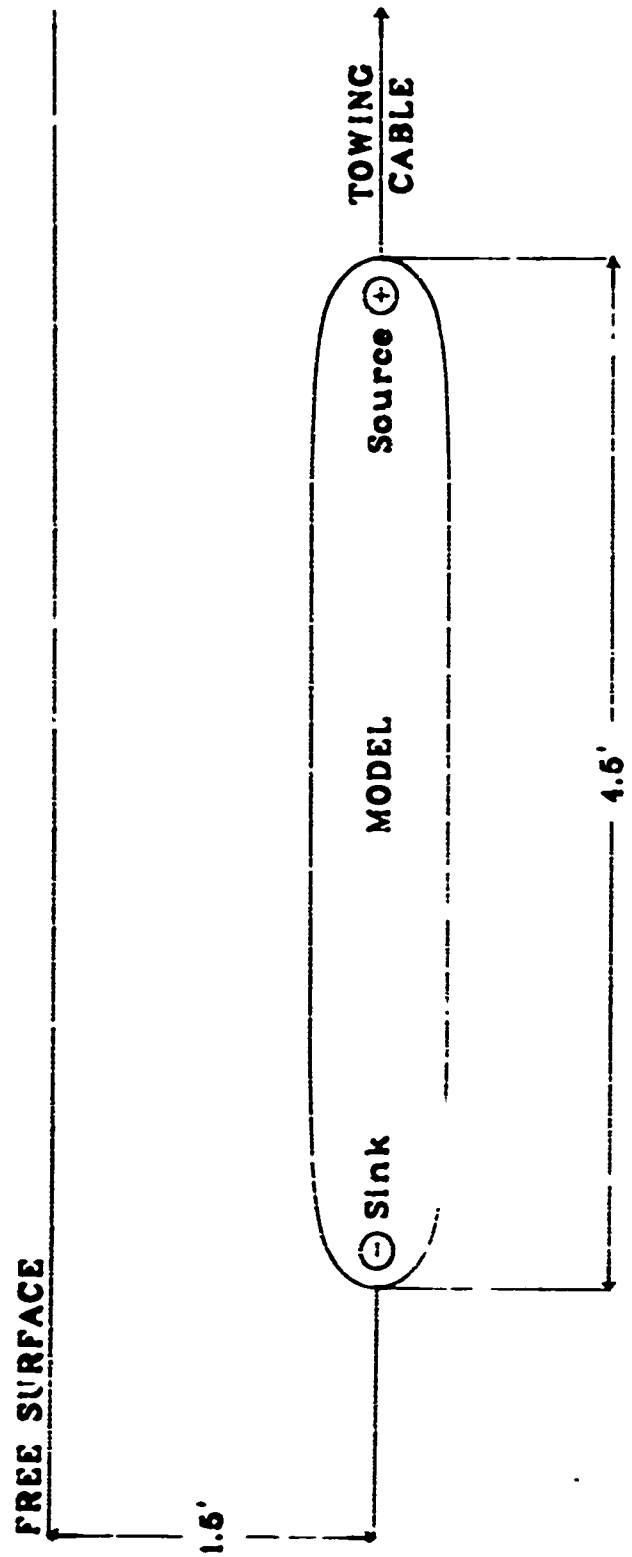
### REFERENCES

1. *The calculation on NORC of source functions for ship waves.*  
A. R. DiDonato, Naval Weapons Laboratory Report No. 1588 (16 April 1958)
2. *Waves due to a submerged body.* B. Yim, Hydronautics, Inc.  
Technical Report No. 231-3 (May 1963)
3. *On the surface wave pattern of submerged bodies started from rest.* C. C. Hsu, Hydronautics, Inc. Technical Report No. 231-7 (April 1965)
4. *A comparison between theoretical and measured waves above a submerged Rankine body.* C. C. Hsu and B. Yim, Hydronautics, Inc. Technical Report No. 231-10 (February 1966)
5. *Computing programs for surface wave trains of point sources.*  
A. V. Hershey, Naval Weapons Laboratory Report No. 1987 (30 June 1965)
6. *On a class of integrals related to those of Raabe and Laplace occurring in the theory of water waves.* R. Barakat, Journal of Mathematics and Physics. 40, 244 (1961)
7. *Modern developments of the theory of wave-making resistance in the non-uniform motion.* H. Maruo. The Society of Naval Architects of Japan, 60th Anniversary Series 2 1 (1957)
8. *Surface effects model.* David Taylor Model Basin Drawing No. E-2298-1, Revision I, dated 12 Jan 1965.
9. *Preliminary Kelvin wake study.* W. Livingston, David Taylor Model Basin Hydromechanics Laboratory Report No. 039-H-01 (December 1964)

10. *Surface waves generated by a submerged Rankine ovoid.* D. A. Shaffer, David Taylor Model Basin Hydromechanics Laboratory Report No. 105-H-01 (October 1965)
11. *Flow and drag formulas for simple quadrics.* A. F. Zahm, NACA Technical Report No. 253 (1927)
12. *Hydrodynamics.* H. Lamb (Dover Publications, New York, 1945)
13. *A Treatise on the Theory of Bessel Functions.* G. N. Watson (Cambridge University Press, 1962)
14. *Preliminary experiments on the real flow field about an axisymmetric Rankine oval.* P. J. Roache. UNDAS-TN-966PR, Department of Aero-Space Engineering, University of Notre Dame, Notre Dame, Indiana. (September 1966)

**APPENDIX A**  
**SCHEMATIC DIAGRAM**

# THE RANKINE OVOID



SCHEMATIC DIAGRAM

$\frac{1}{10}$  Scale

**APPENDIX B**

**TABLES I to V**

TABLE I

Speeds for which Wave Profiles were Computed

$U(\text{ft})/(\text{sec})$	$x_0(\text{ft})^{-1}$	$\lambda(\text{ft})$
3.7760	2.2565	2.7845
4.6247	1.5043	4.1768
6.0	0.8933	7.0337
7.3	0.6035	10.4112
9.0	0.3970	15.8267
10.0	0.3216	19.5373

TABLE II

Offsets for Rankine Ovoid  
with Length to Diameter Ratio of 7

$x$ (in)	$r$ (in)
0.000	3.857
2.592	3.857
5.184	3.854
7.776	3.850
10.386	3.842
12.960	3.830
15.252	3.809
18.144	3.757
20.724	3.642
21.600	3.570
23.328	3.316
25.200	2.669
25.920	2.182
26.400	1.685
27.000	0.000

TABLE III

Maximum Effect of Linearization on Surface Elevation

$U(\text{ft})/(\text{sec})$	Error (ft)
3.7760	.0002
4.6247	.0006
6.0	.0017
7.3	.0018
9.0	.0018
10.0	.0017

TABLE IV

Percent Decrease in Amplitude for 1.5" Increase in Depth

$U(\text{ft})/(\text{sec})$	% Decrease
3.7760	28
4.6247	19
6.0	11
7.3	$7\frac{1}{2}$
9.0	5
10.0	4

TABLE V

Times of Termination of Steady Wave Train

Distance (ft)	Speed (ft)/(sec)			
	6.0	7.3	9.0	10.0
	time (sec)			
48	8	7	5	5
63	11	9	7	6
95	16	13	11	10
133	22	18	15	13
187	31	26	21	19

## APPENDIX C

Plots of Elevation  $E$  (ft) versus Time  $T$  (sec)

### NOTES

1. Figures 1 to 24 refer to 133 ft of travel.
2. Figures 25 to 28 refer to 187 ft of travel.
3. Dotted lines represent measured elevations in the transient wave train of a Rankine ovoid.
4. Solid lines represent computed elevations in the steady state wave train of a source and sink.

FIGURE 1  
SURFACE ELEVATION

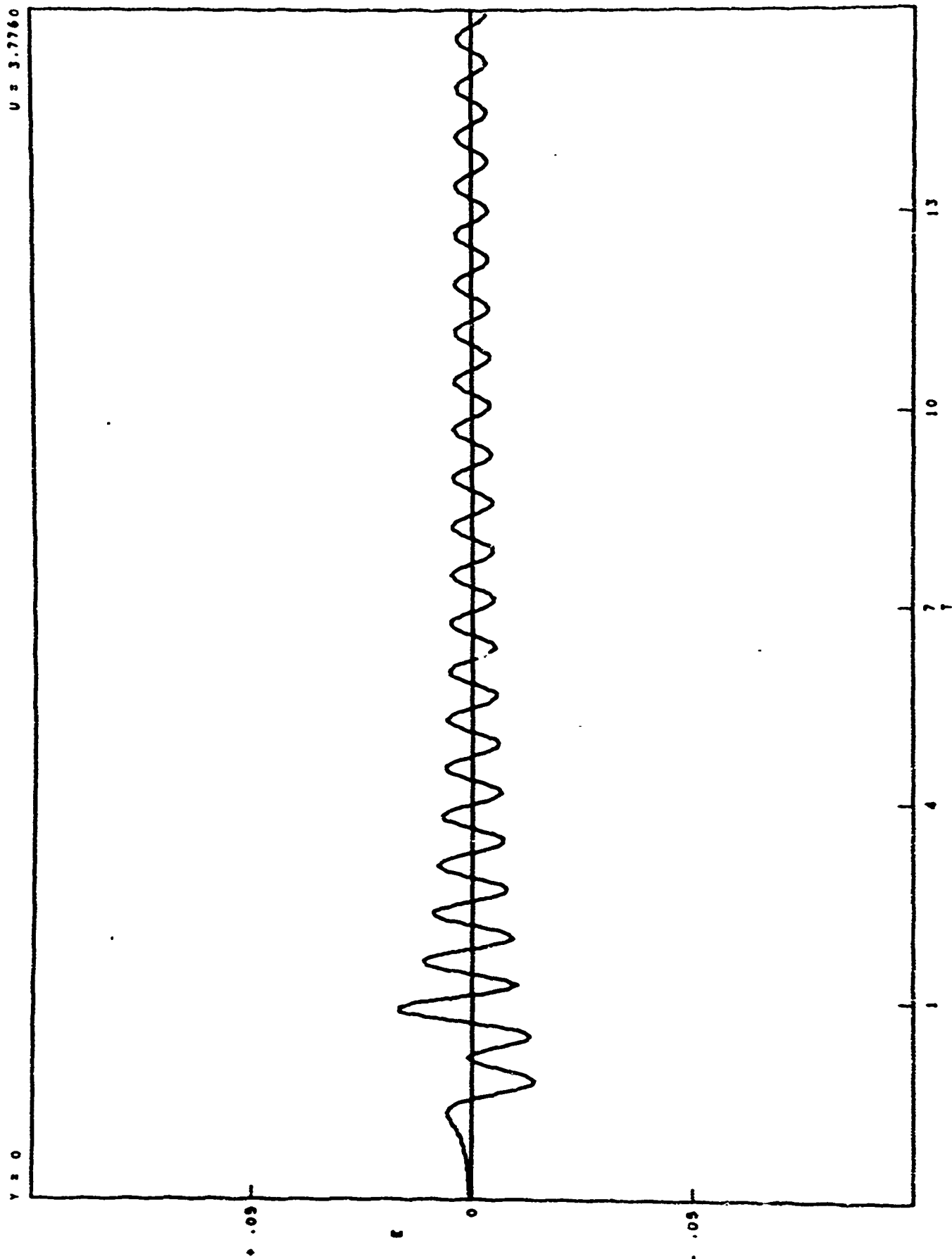


FIGURE 2  
SURFACE ELEVATION

FIGURE 2  
SURFACE ELEVATION

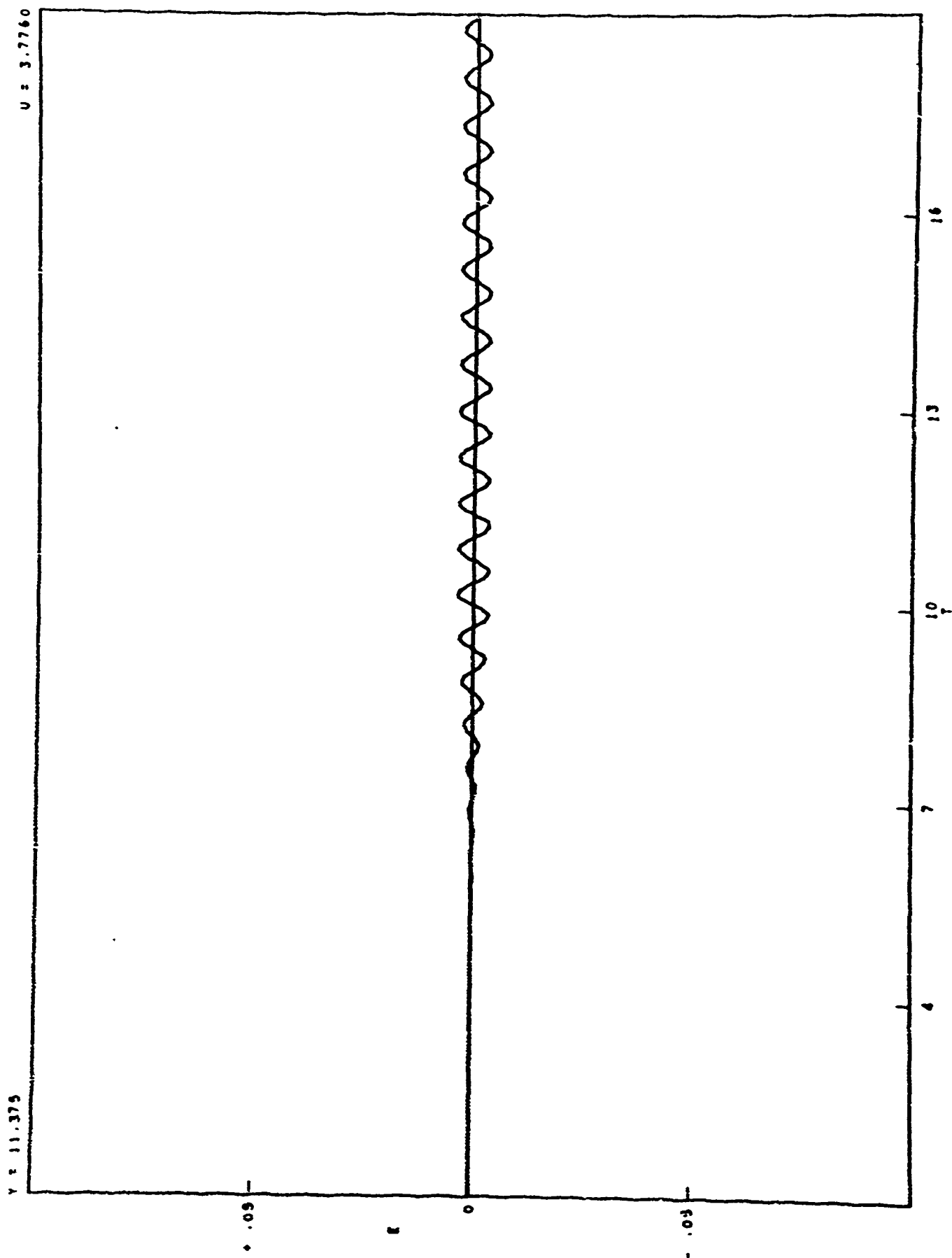


FIGURE 3  
SURFACE ELEVATION

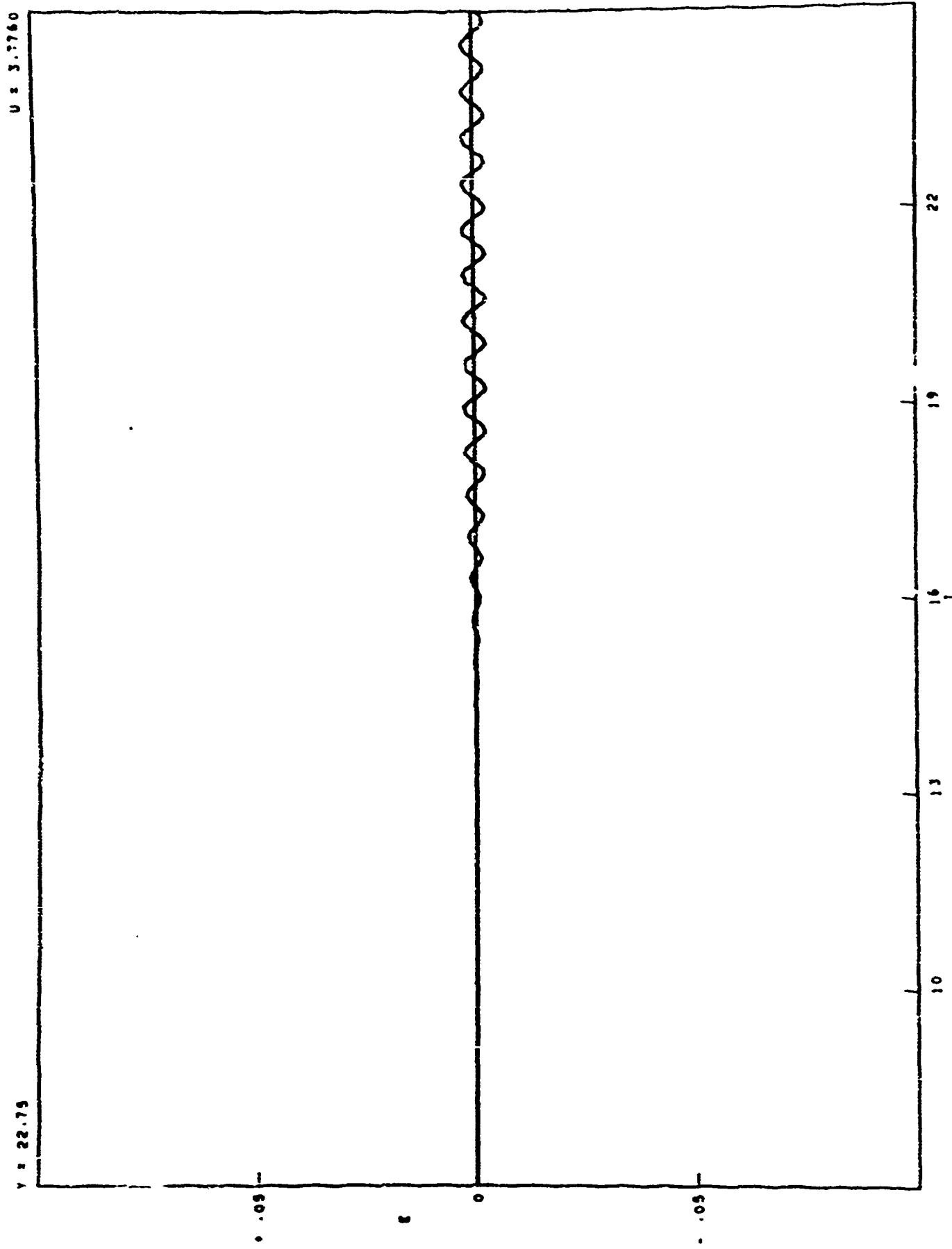


FIGURE 4  
SURFACE ELEVATION

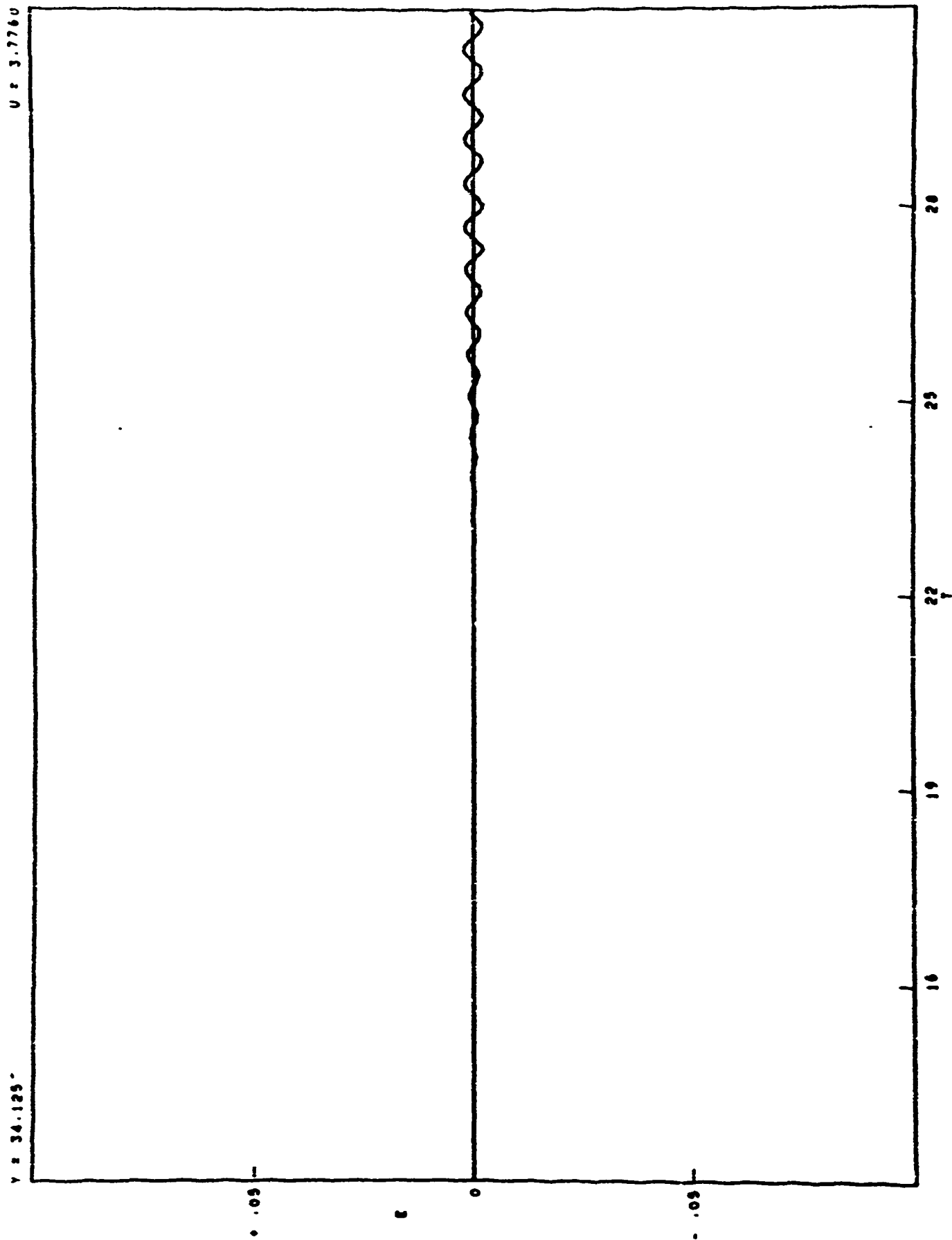


FIGURE 9  
SURFACE ELEVATION

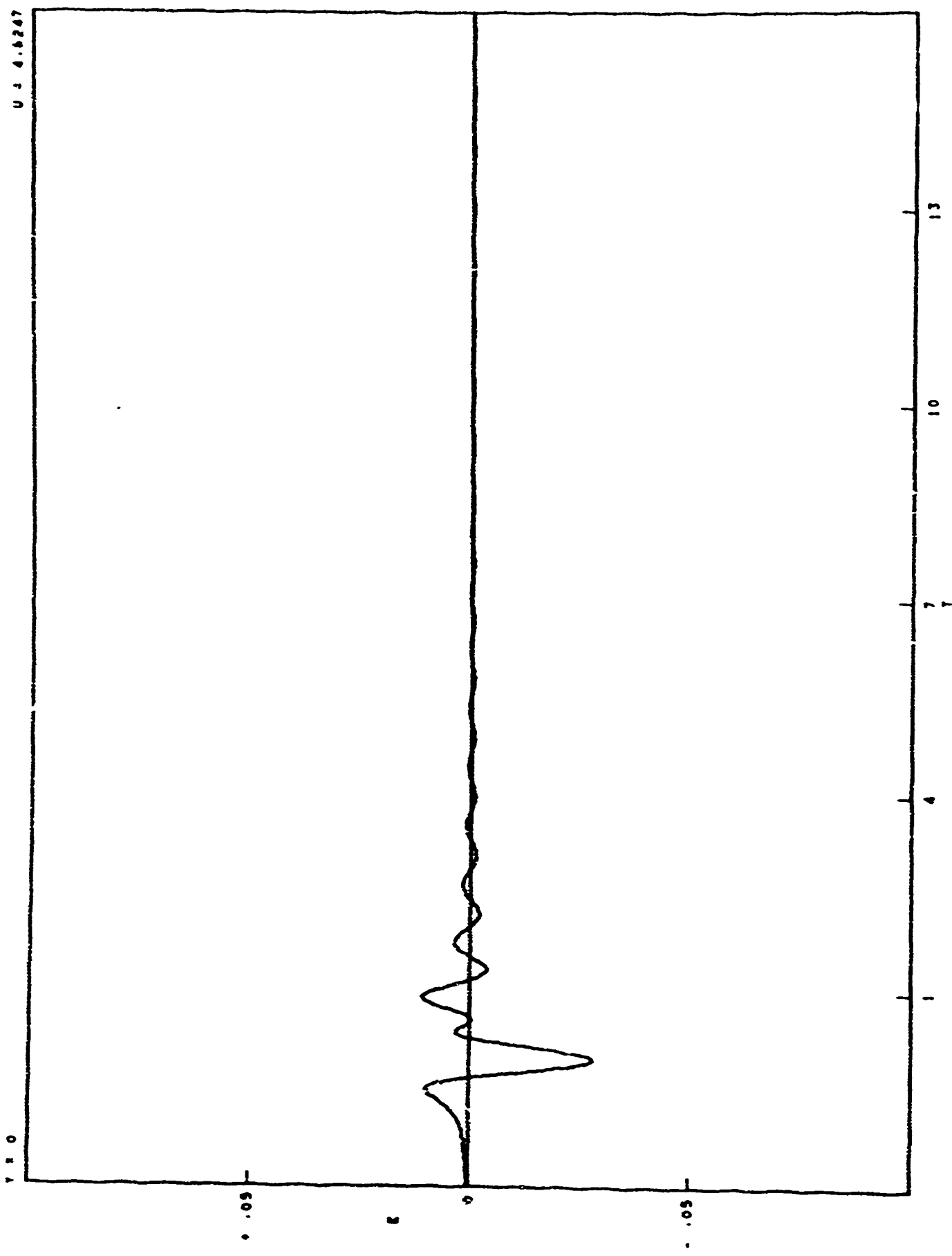


FIGURE 6  
SURFACE ELEVATION

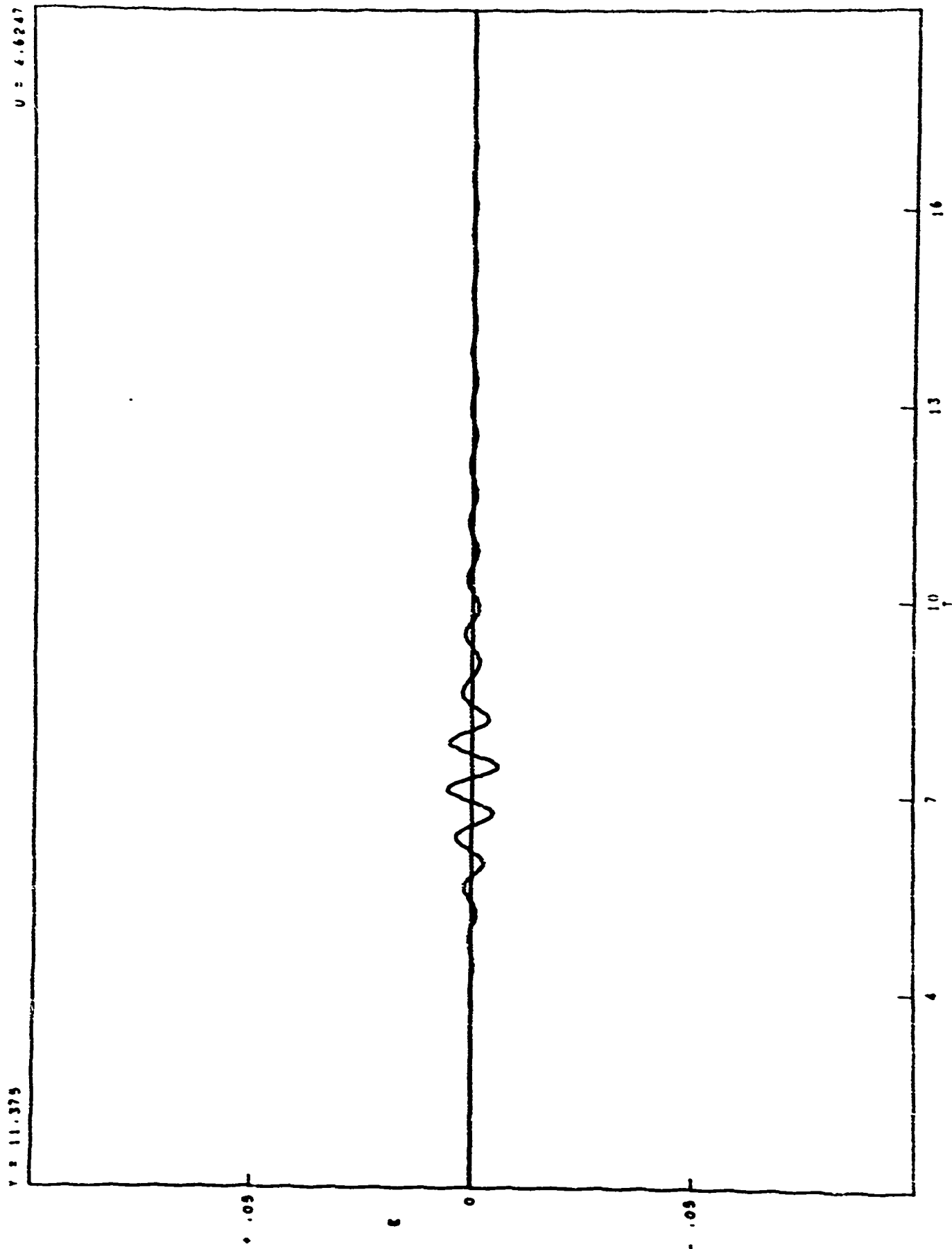


FIGURE 7  
SURFACE ELEVATION

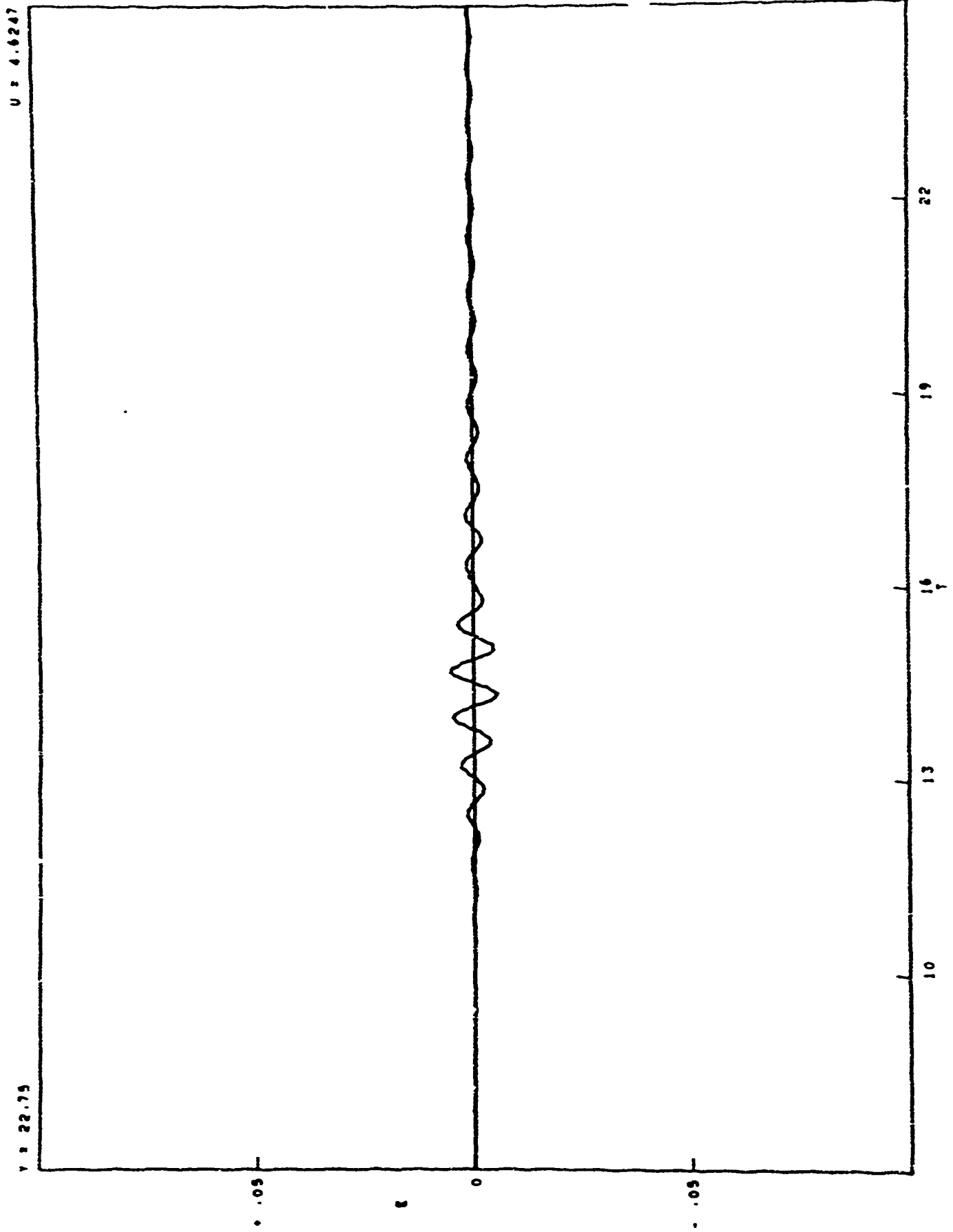


FIGURE 6  
SURFACE ELEVATION

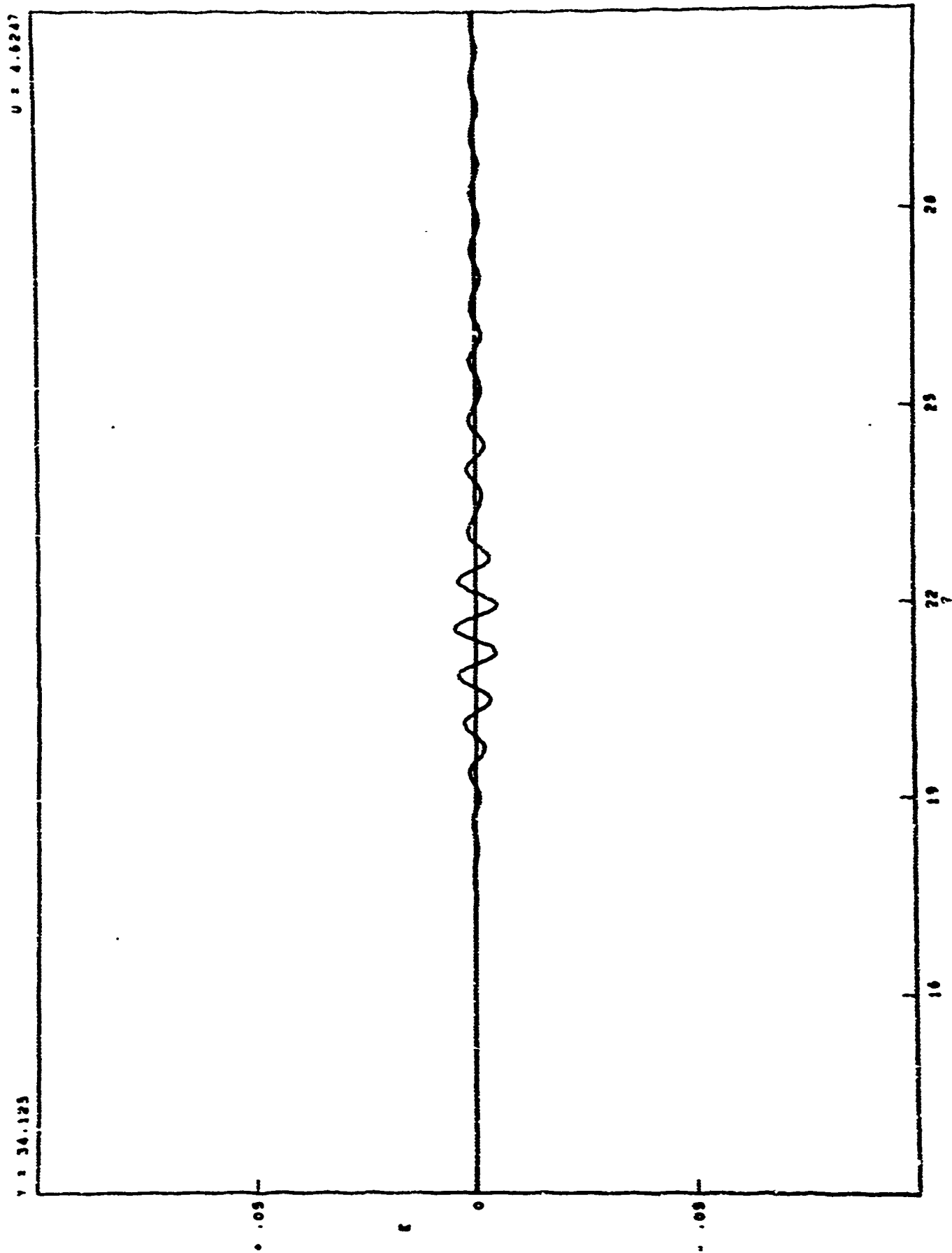


FIGURE 9  
SURFACE ELEVATION

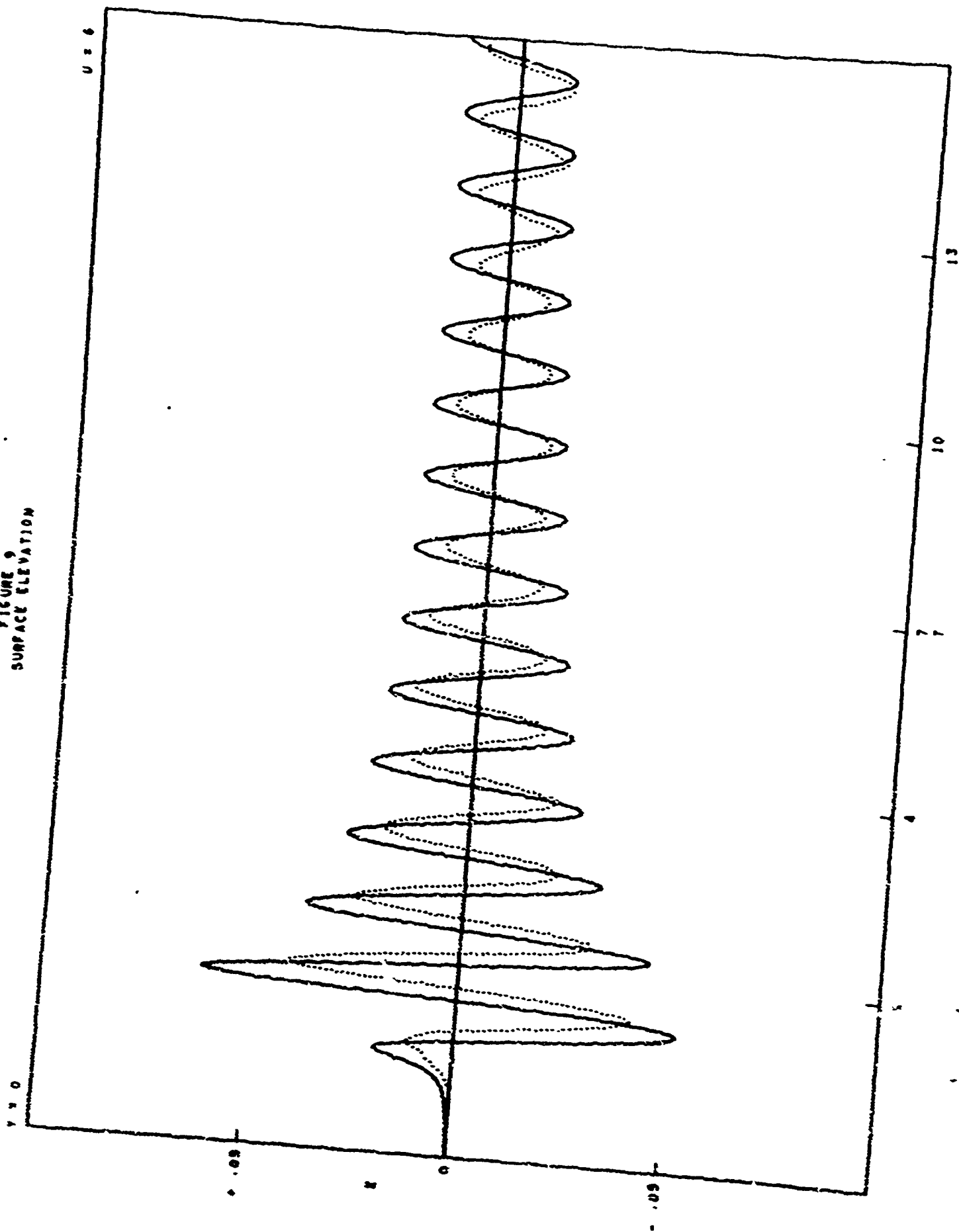


FIGURE 10  
SURFACE ELEVATION

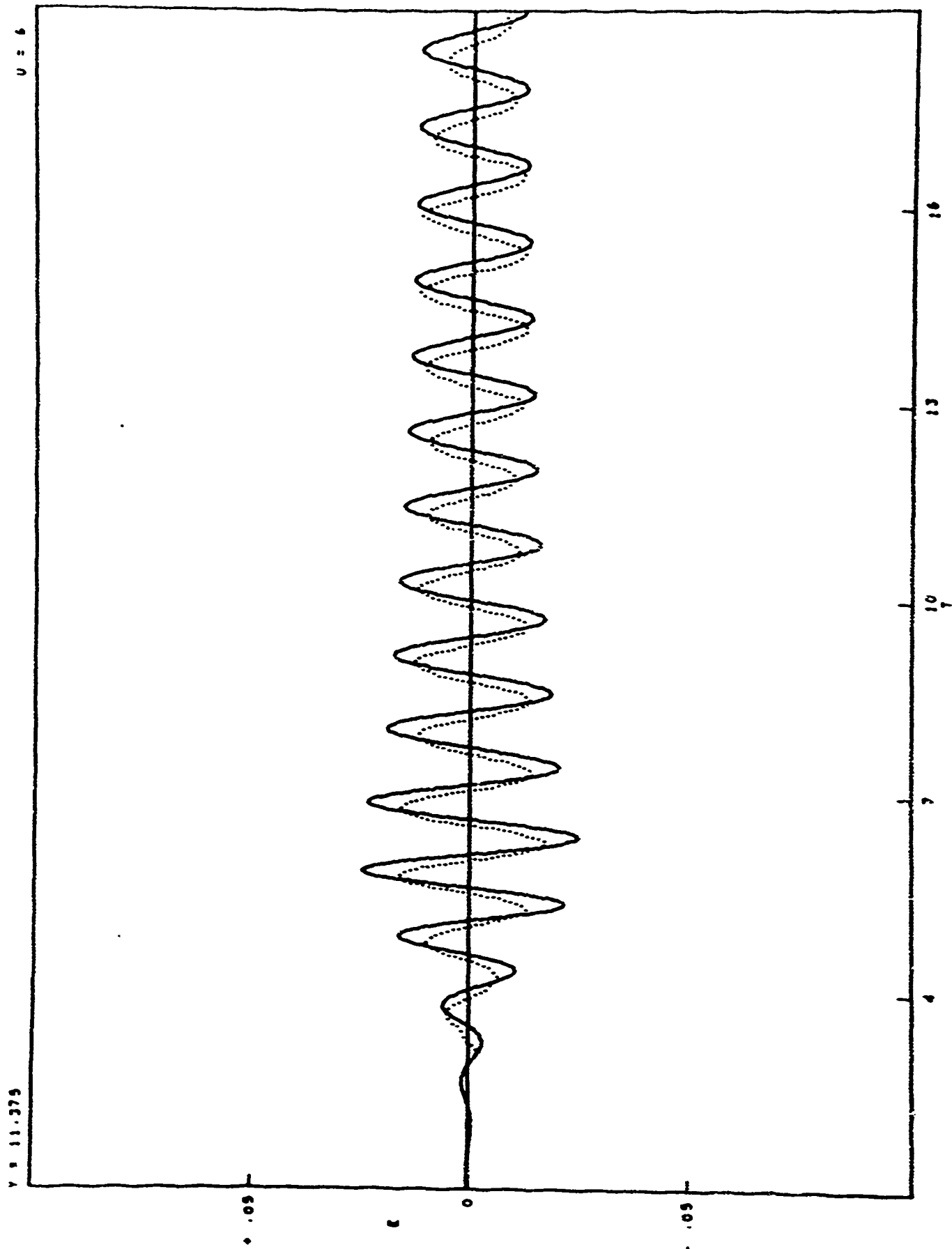


FIGURE 11  
SURFACE ELEVATION

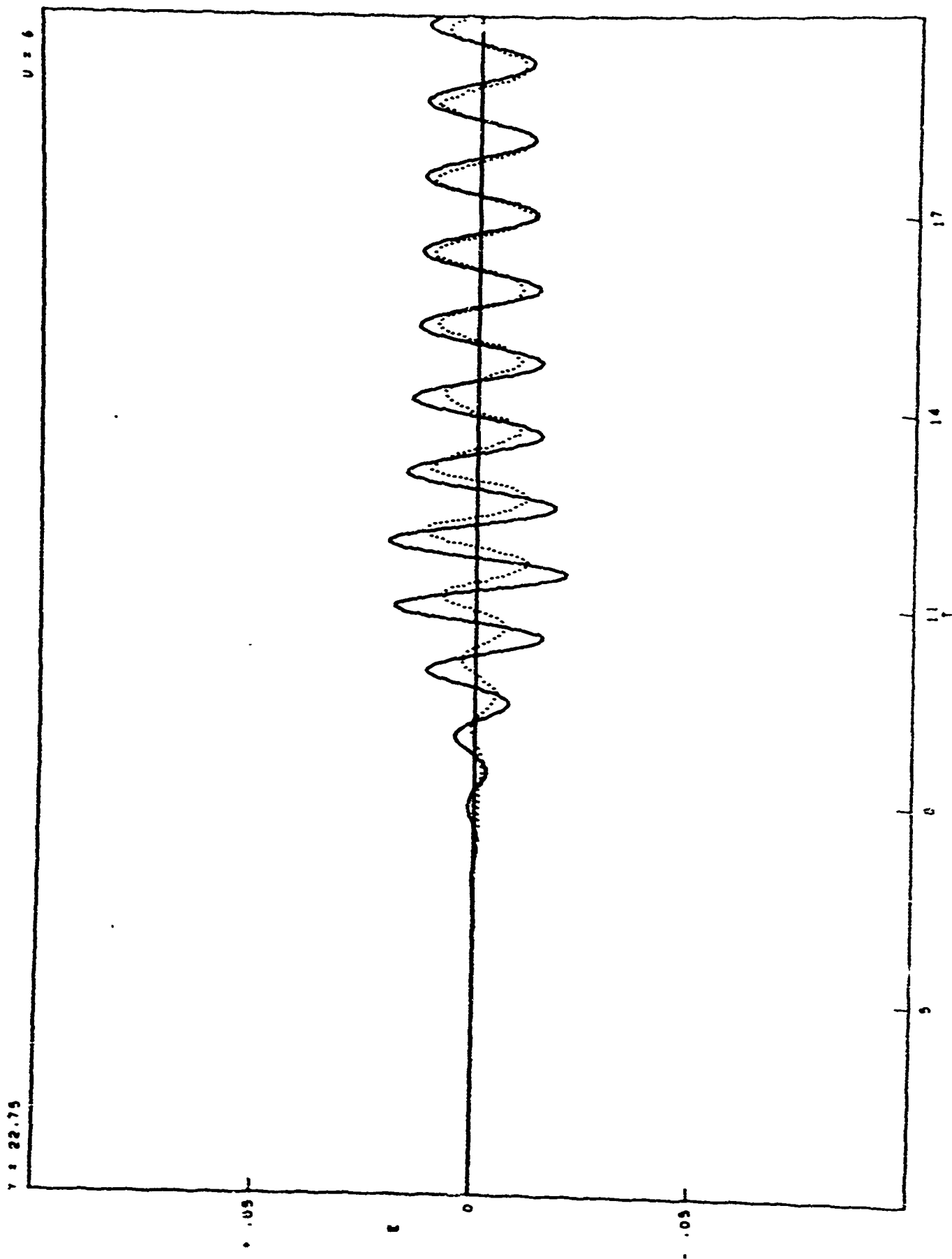


FIGURE 12  
SURFACE ELEVATION

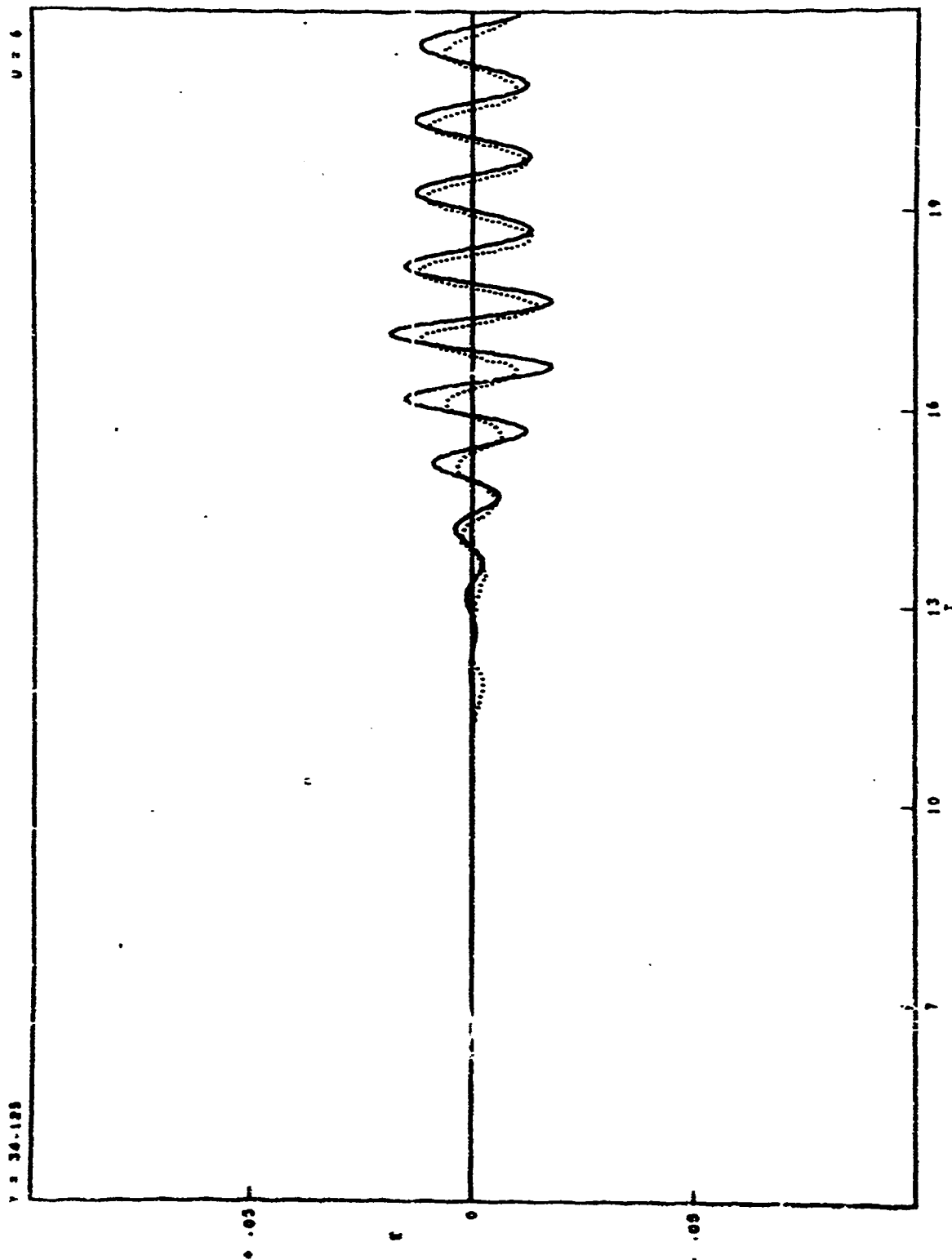


FIGURE 13  
SURFACE ELEVATION

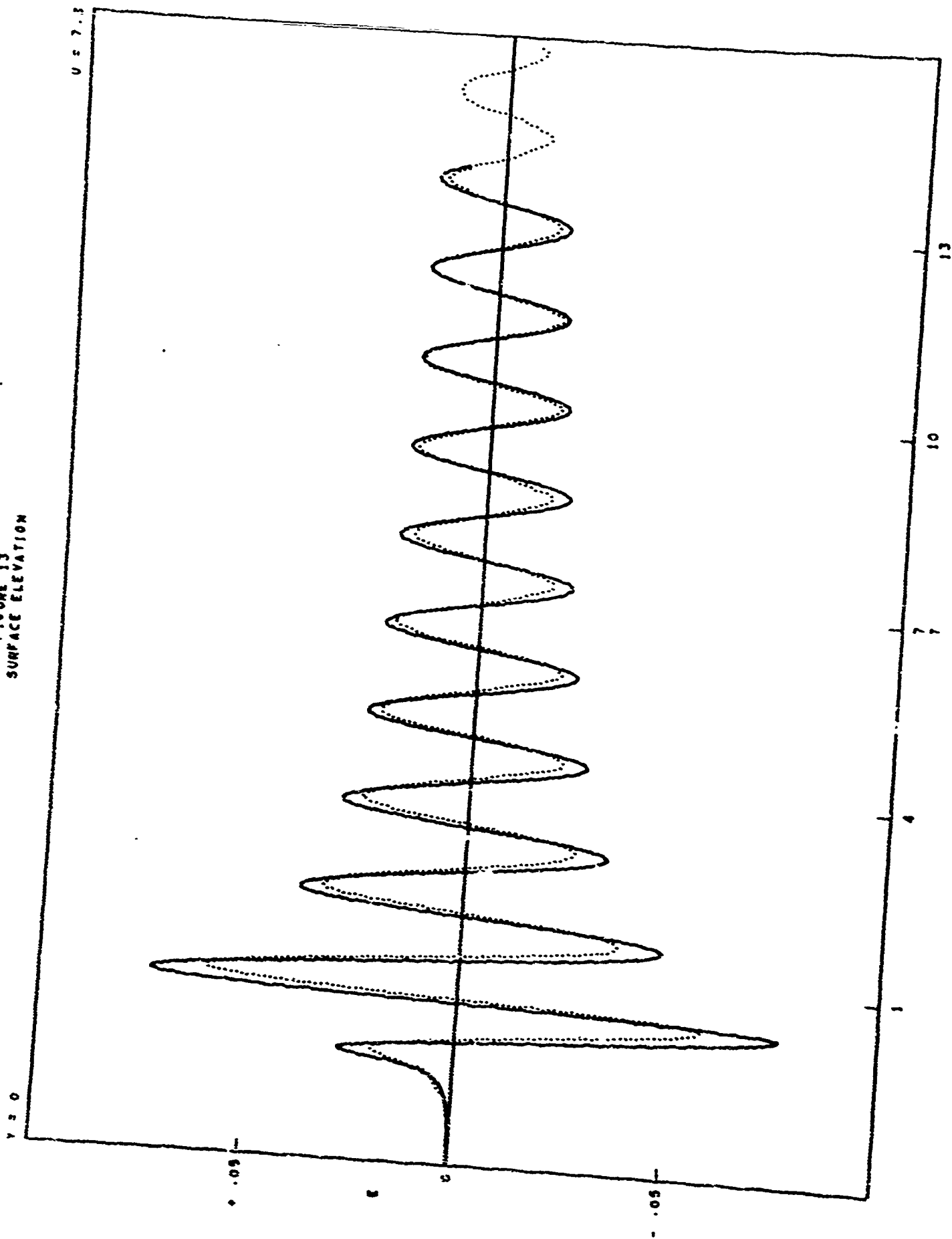


FIGURE 14  
SURFACE ELEVATION

Y = 11.375

U = 7.3

FIGURE 14  
SURFACE ELEVATION

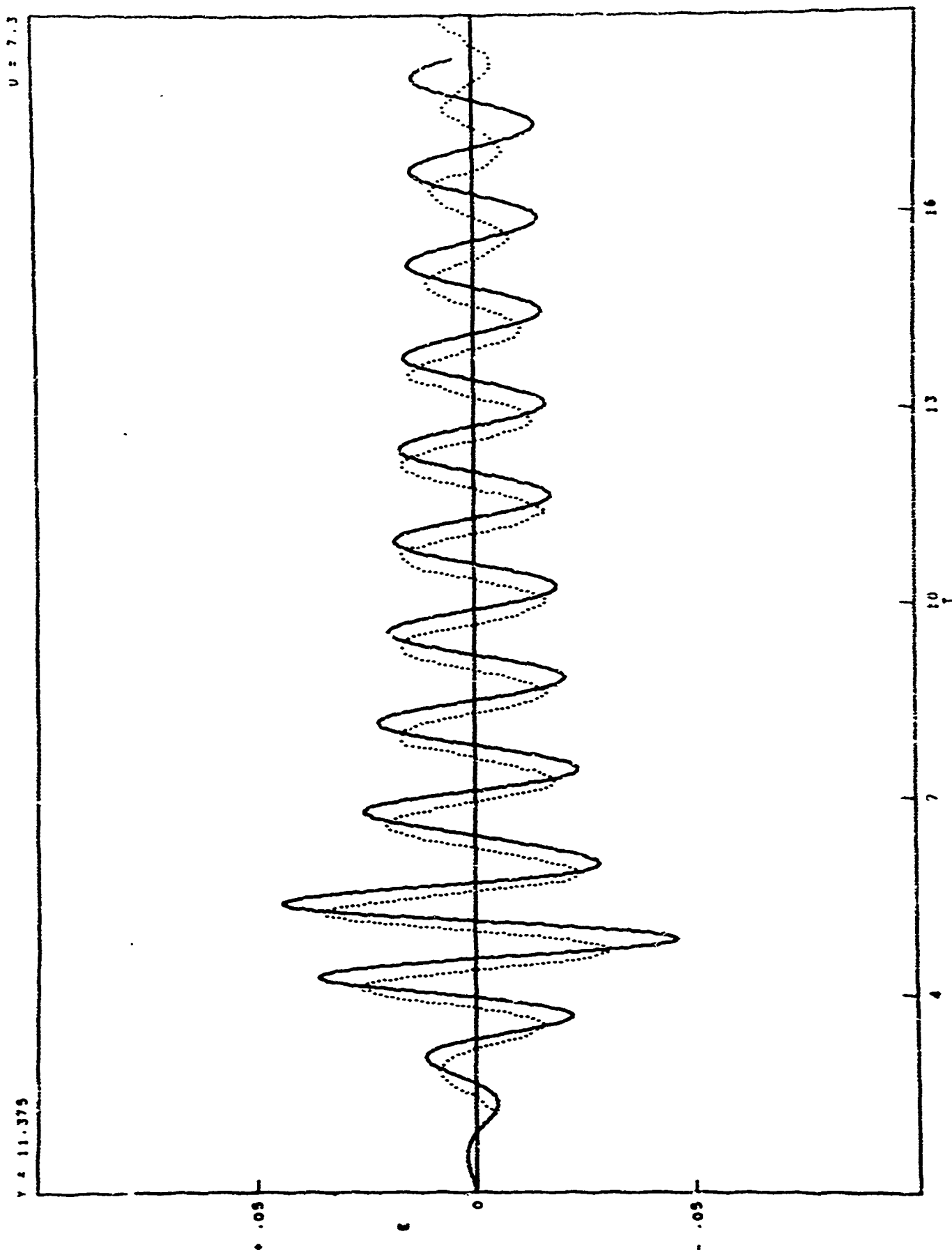


FIGURE 15  
SURFACE ELEVATION

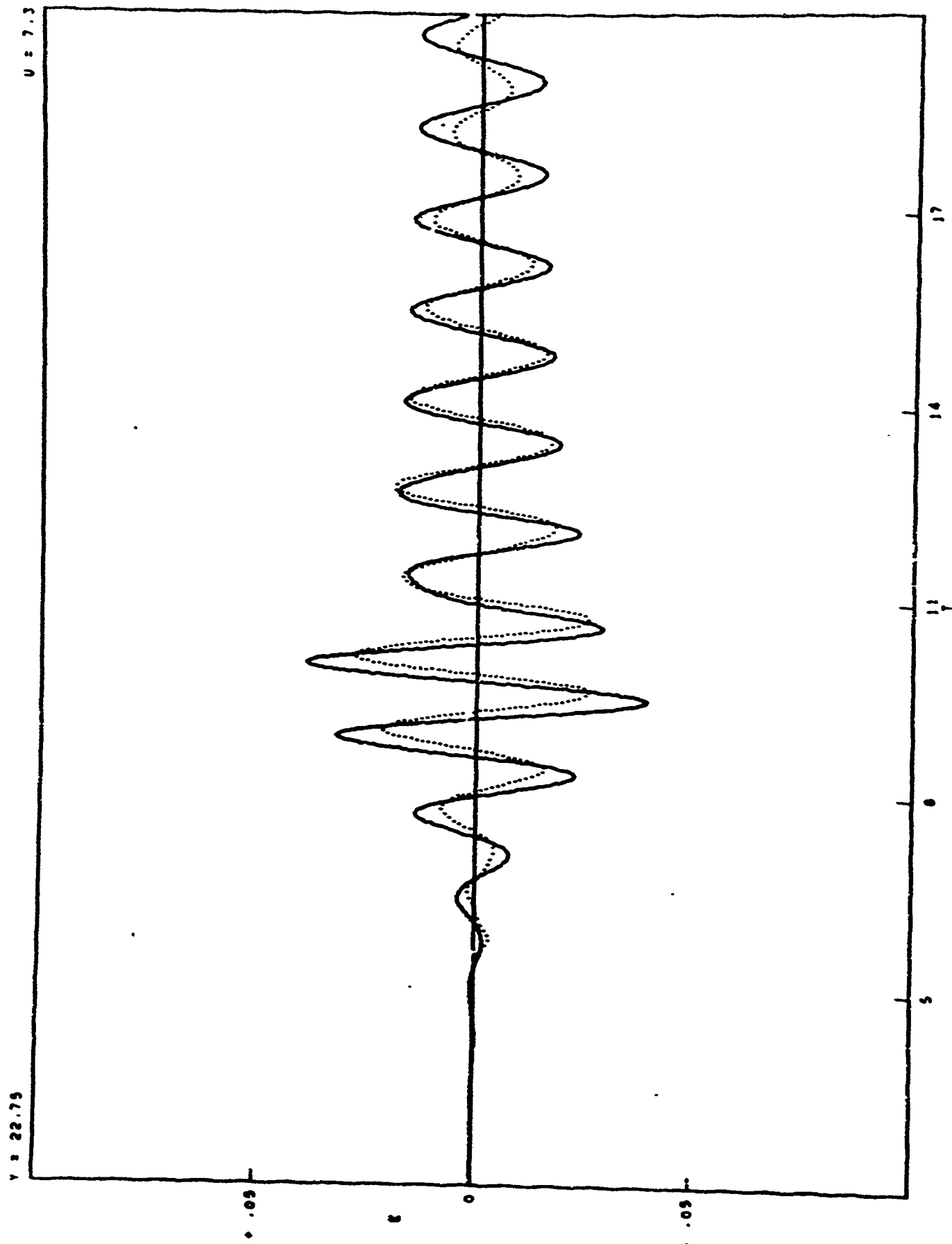


FIGURE 16  
SURFACE ELEVATION

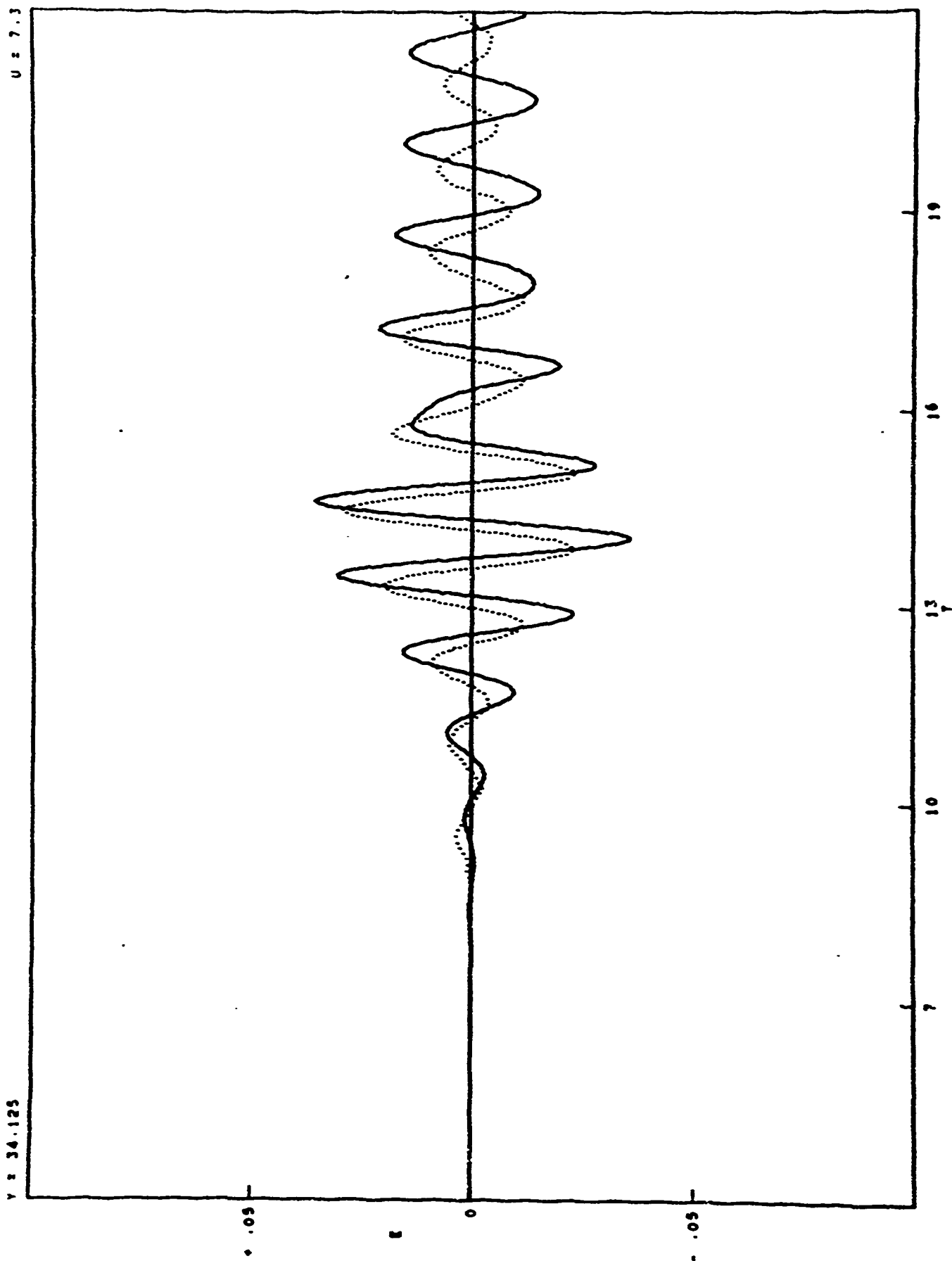


FIGURE 17  
SURFACE ELEVATION

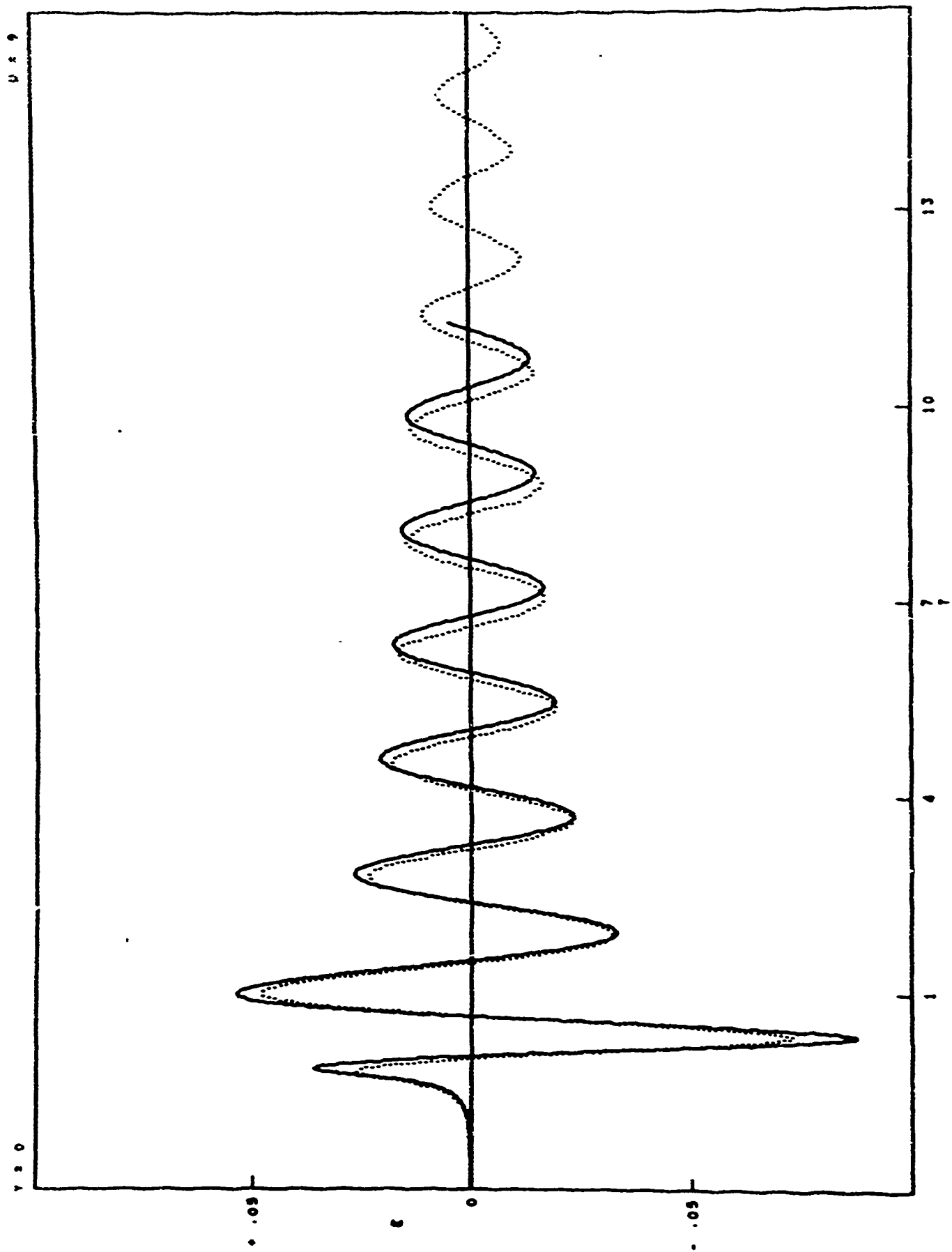


FIGURE 10  
SURFACE ELEVATION

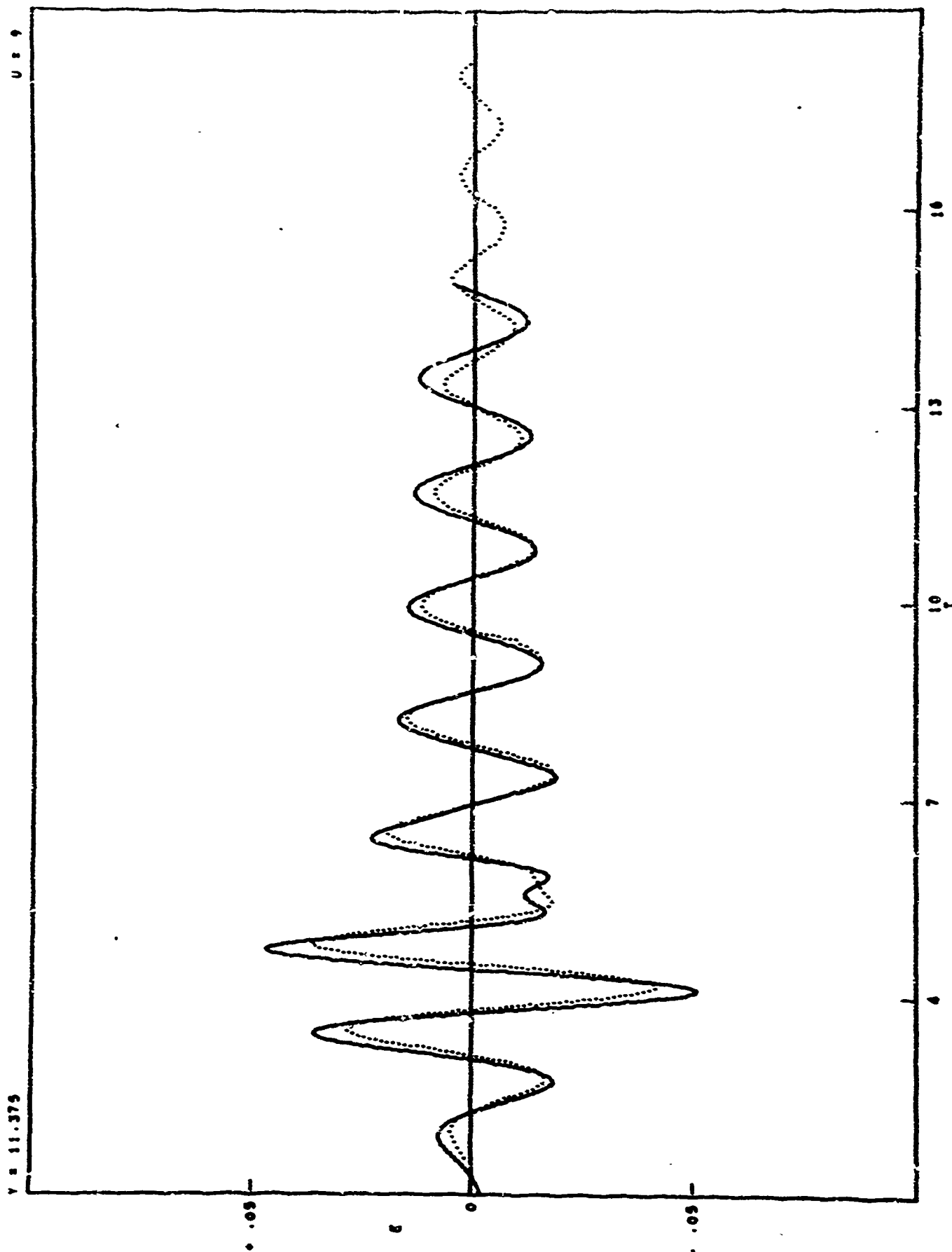


FIGURE 19  
SURFACE ELEVATION

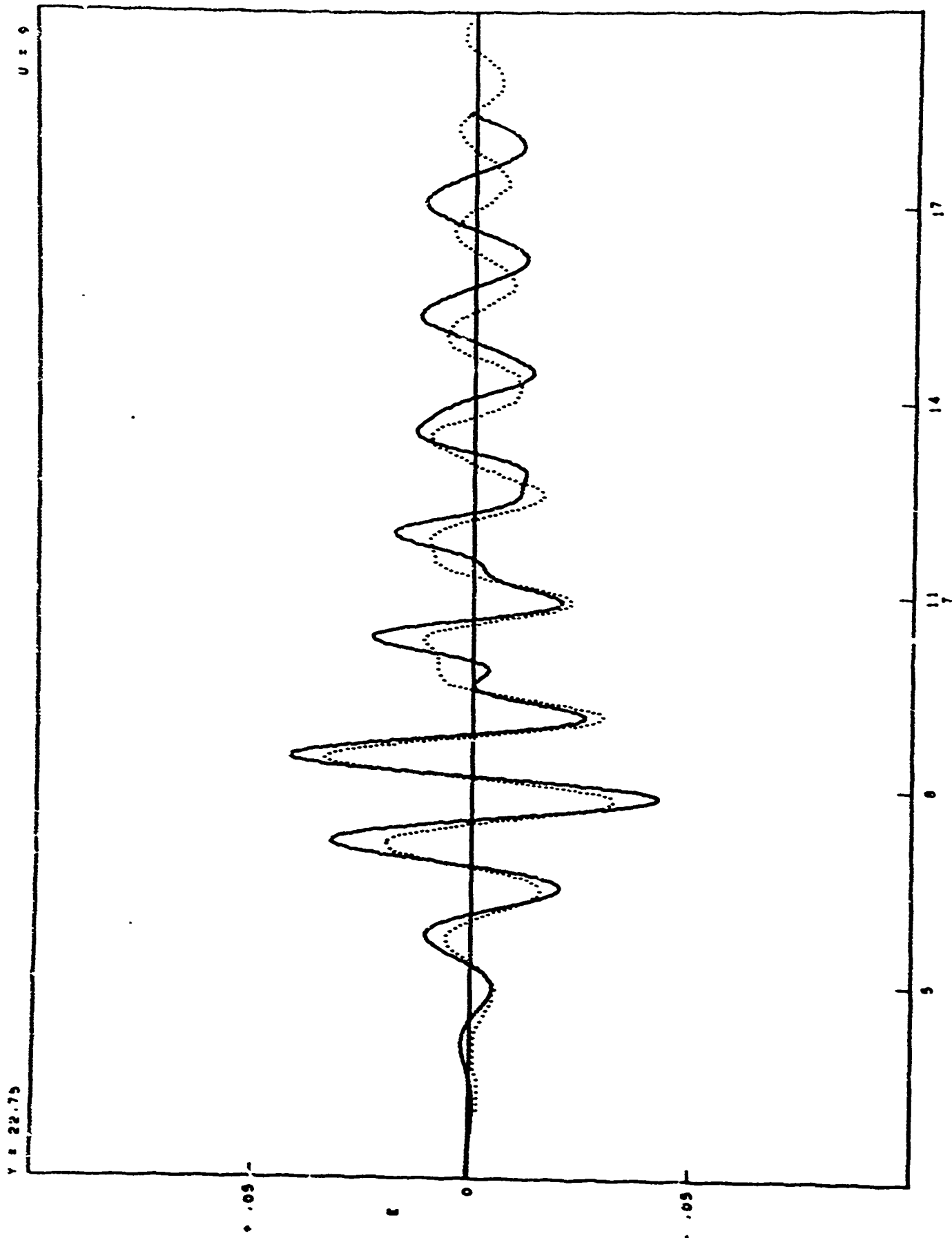


FIGURE 20  
SURFACE ELEVATION

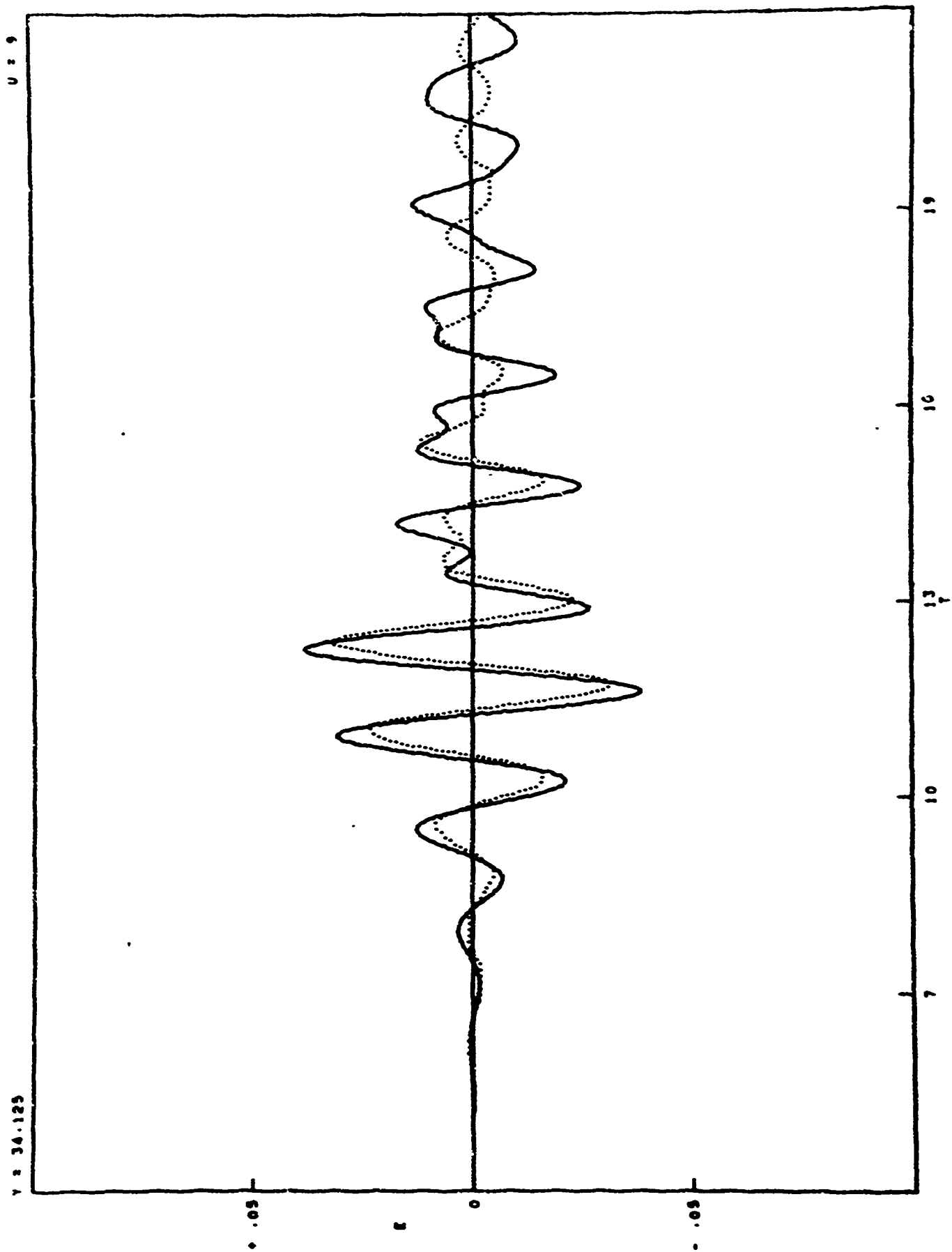


FIGURE 21  
SURFACE ELEVATION

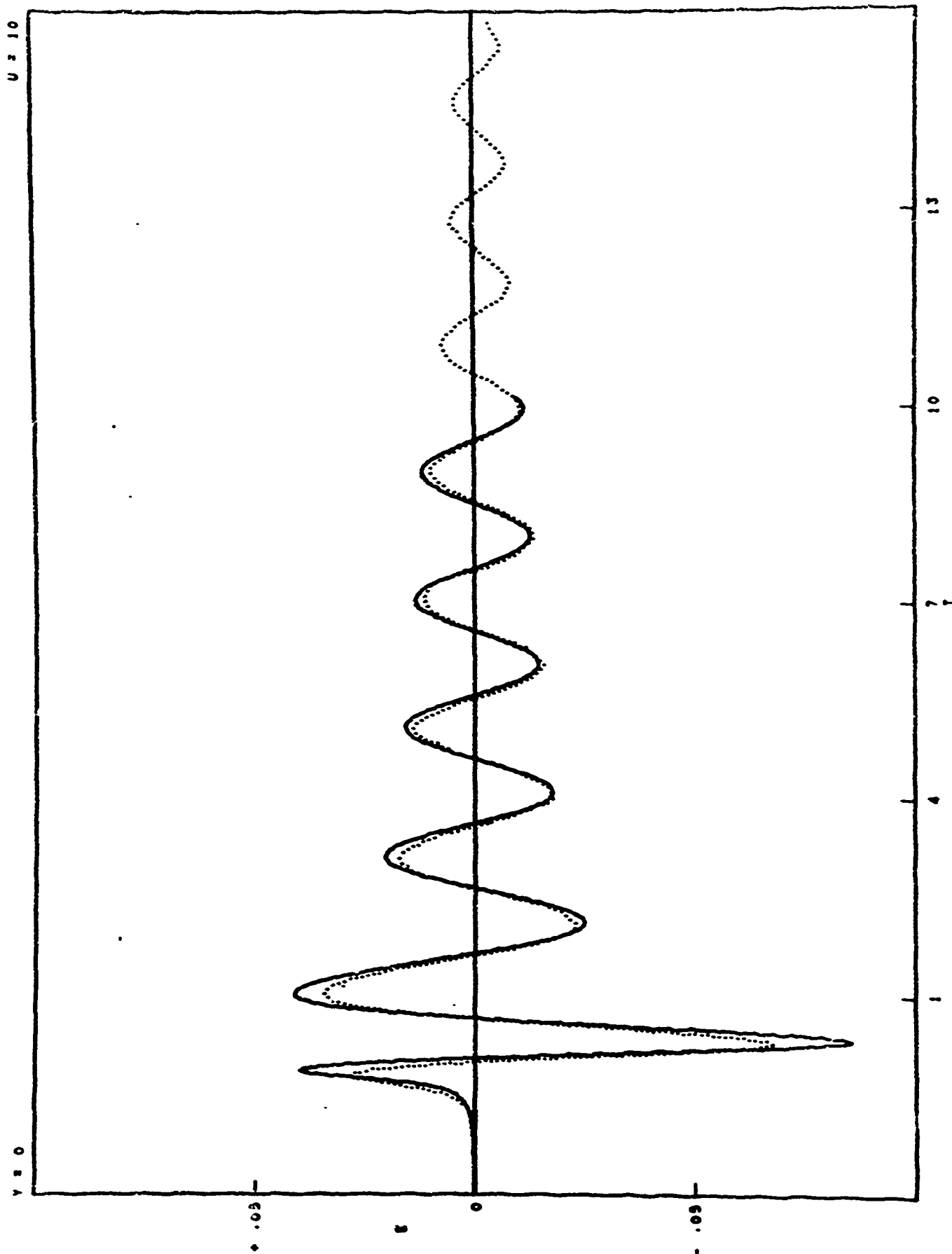


FIGURE 22  
SURFACE ELEVATION

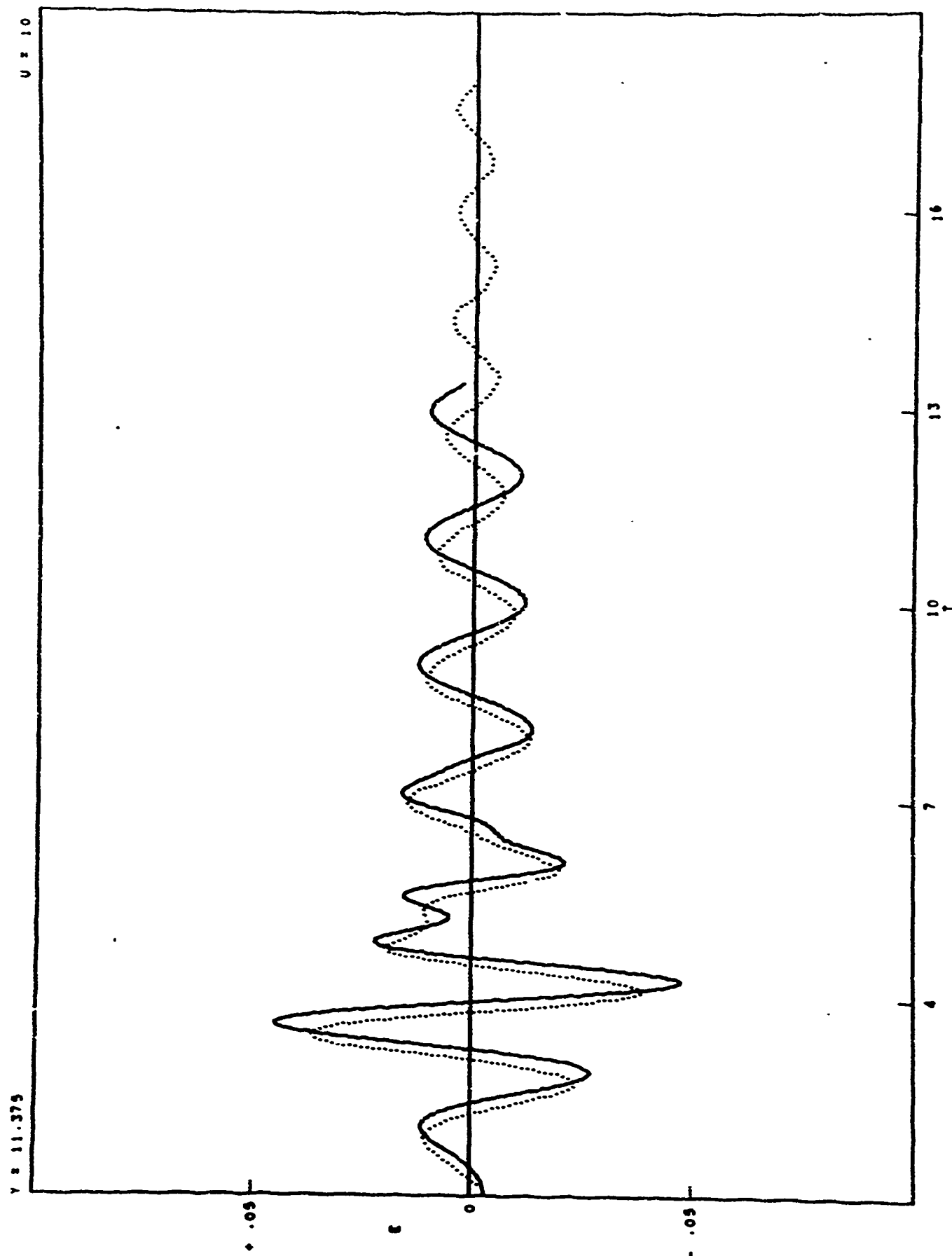


FIGURE 23  
SURFACE ELEVATION

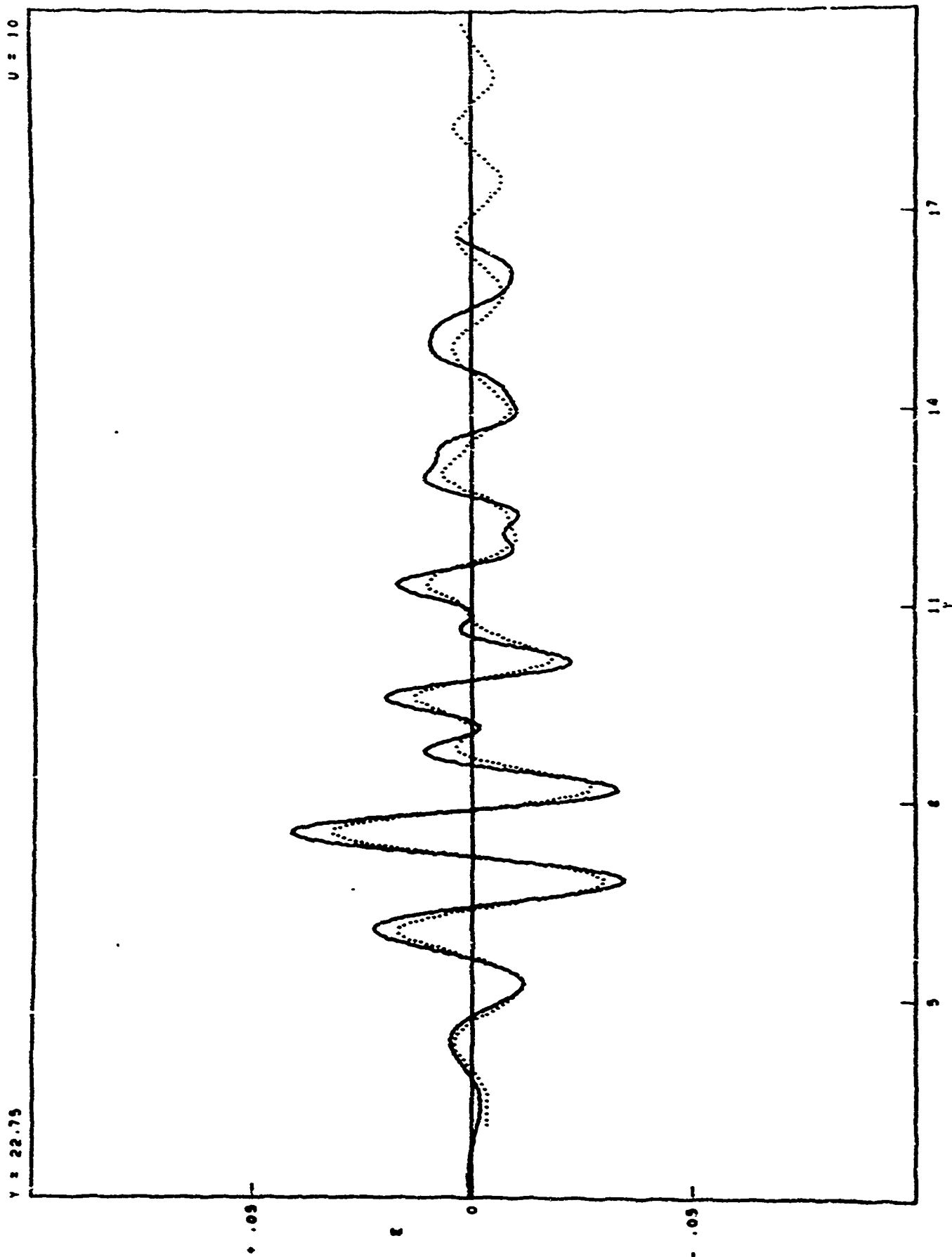


FIGURE 24  
SURFACE ELEVATION

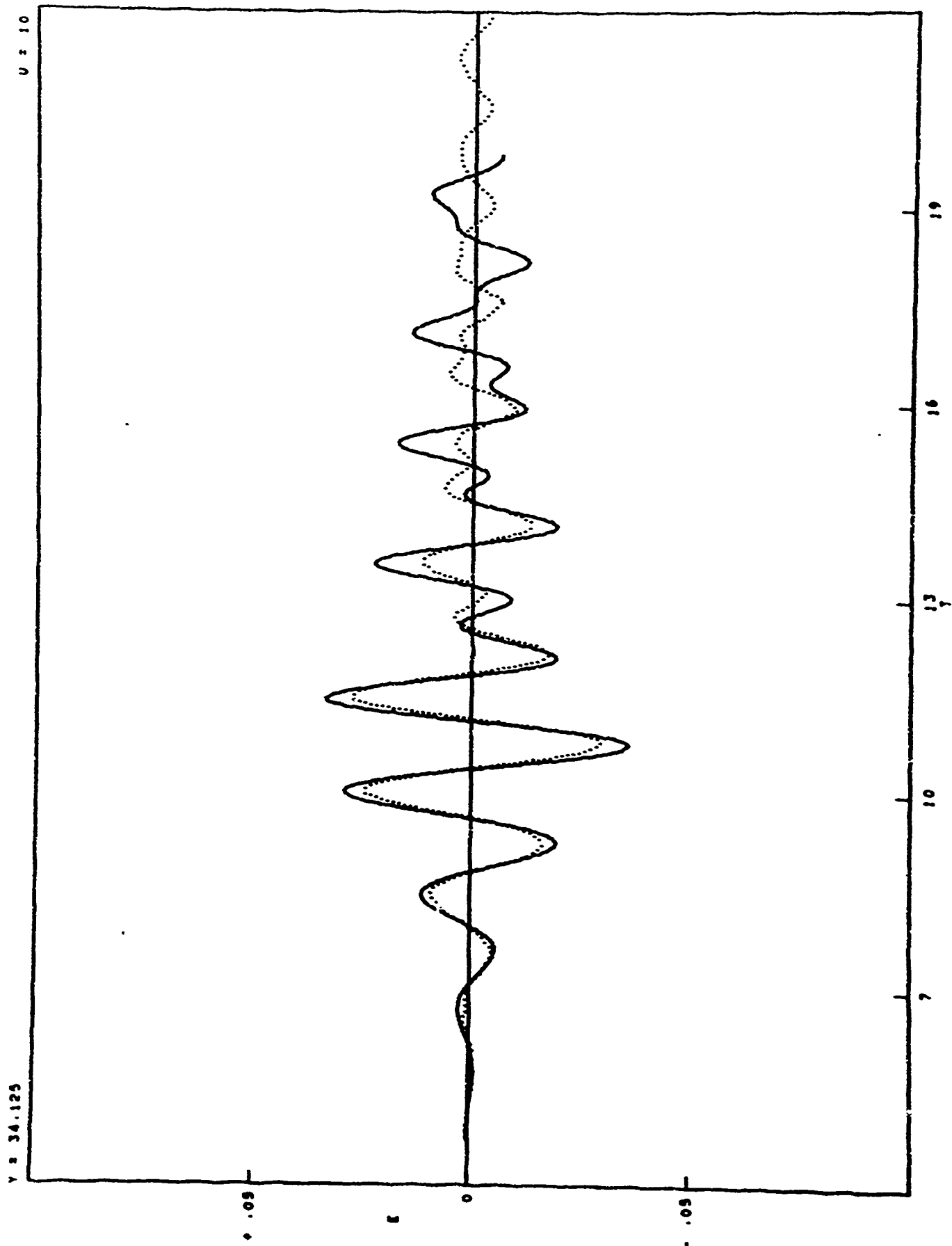


FIGURE 25  
SURFACE ELEVATION

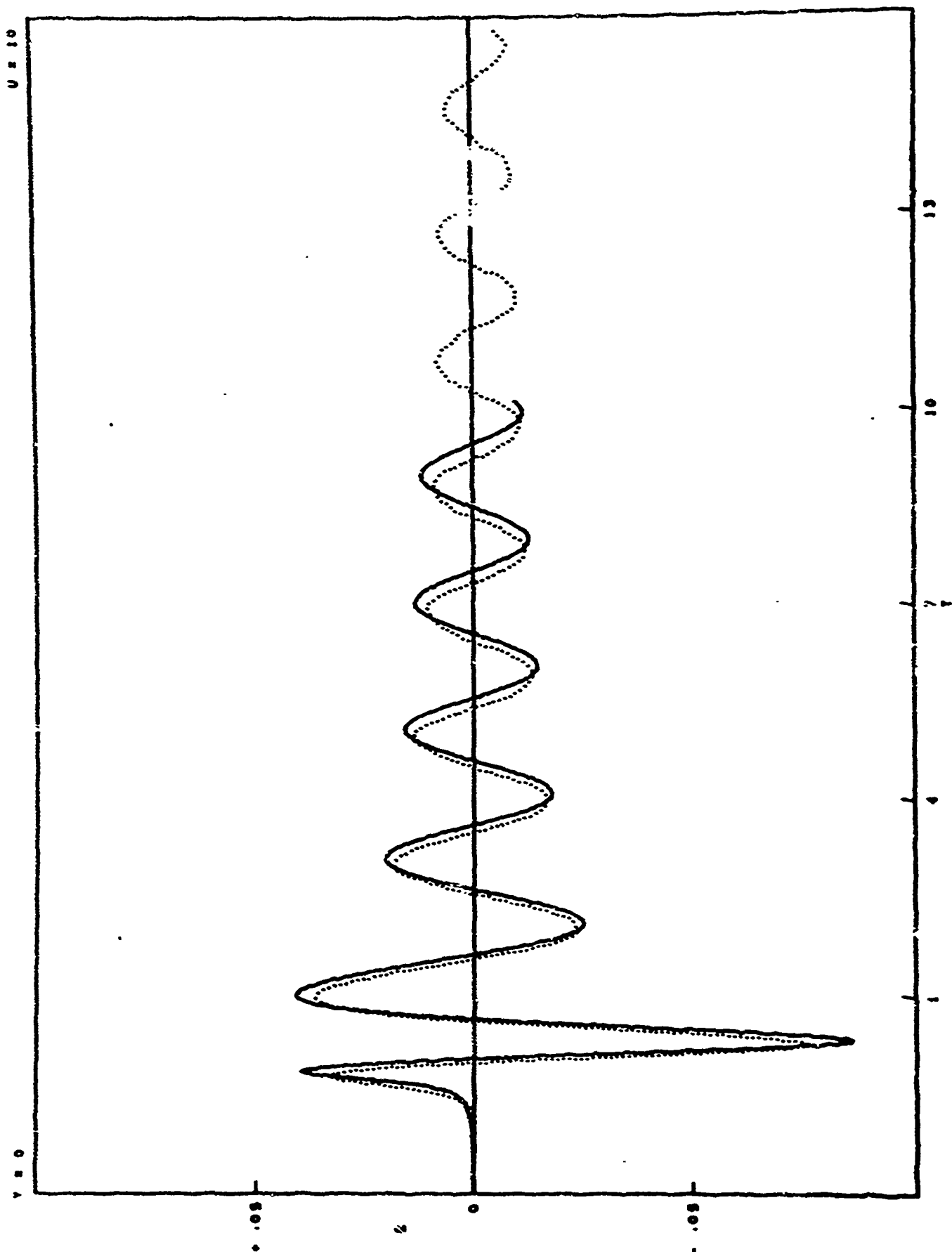


FIGURE 26  
SURFACE ELEVATION

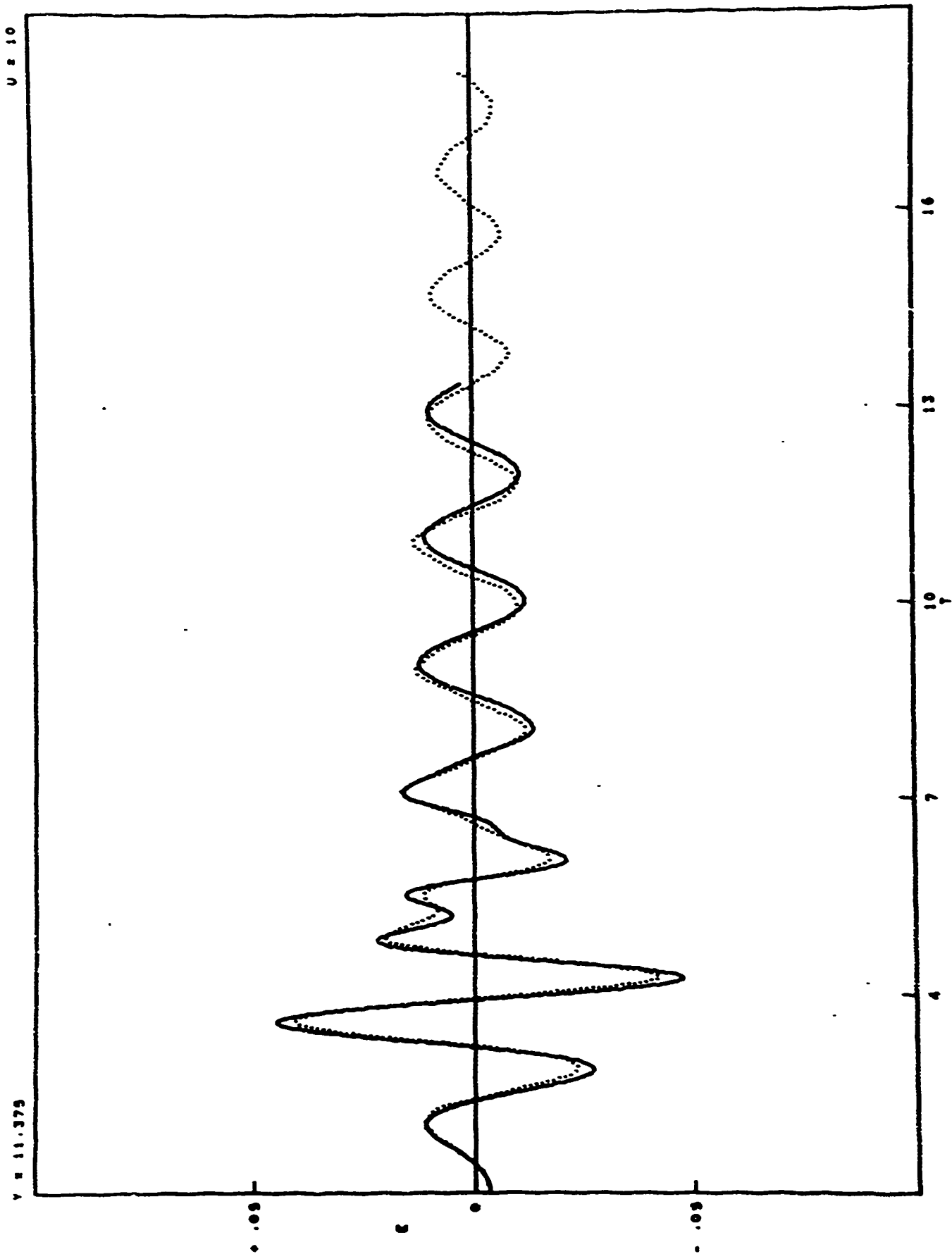


FIGURE 27  
SURFACE ELEVATION

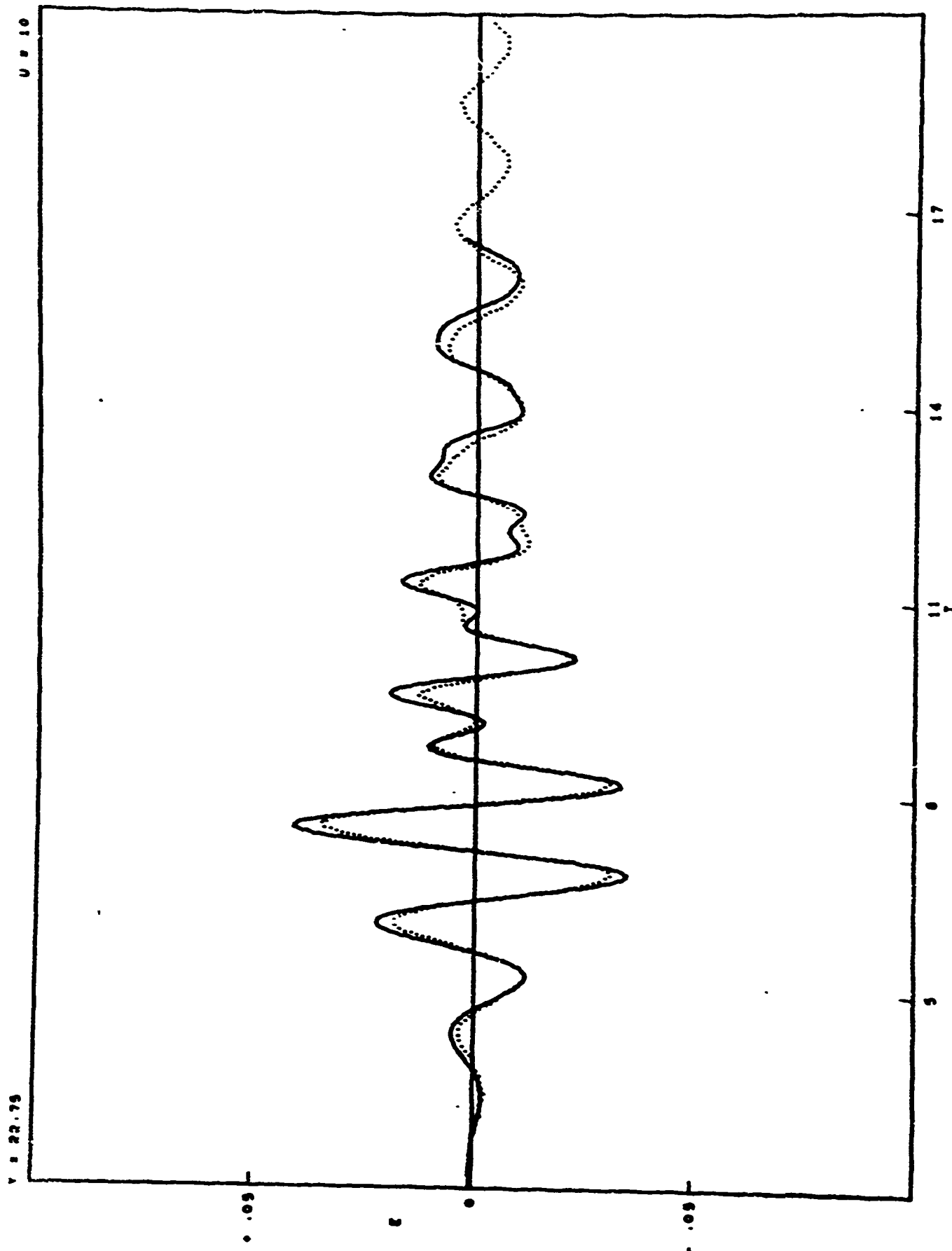
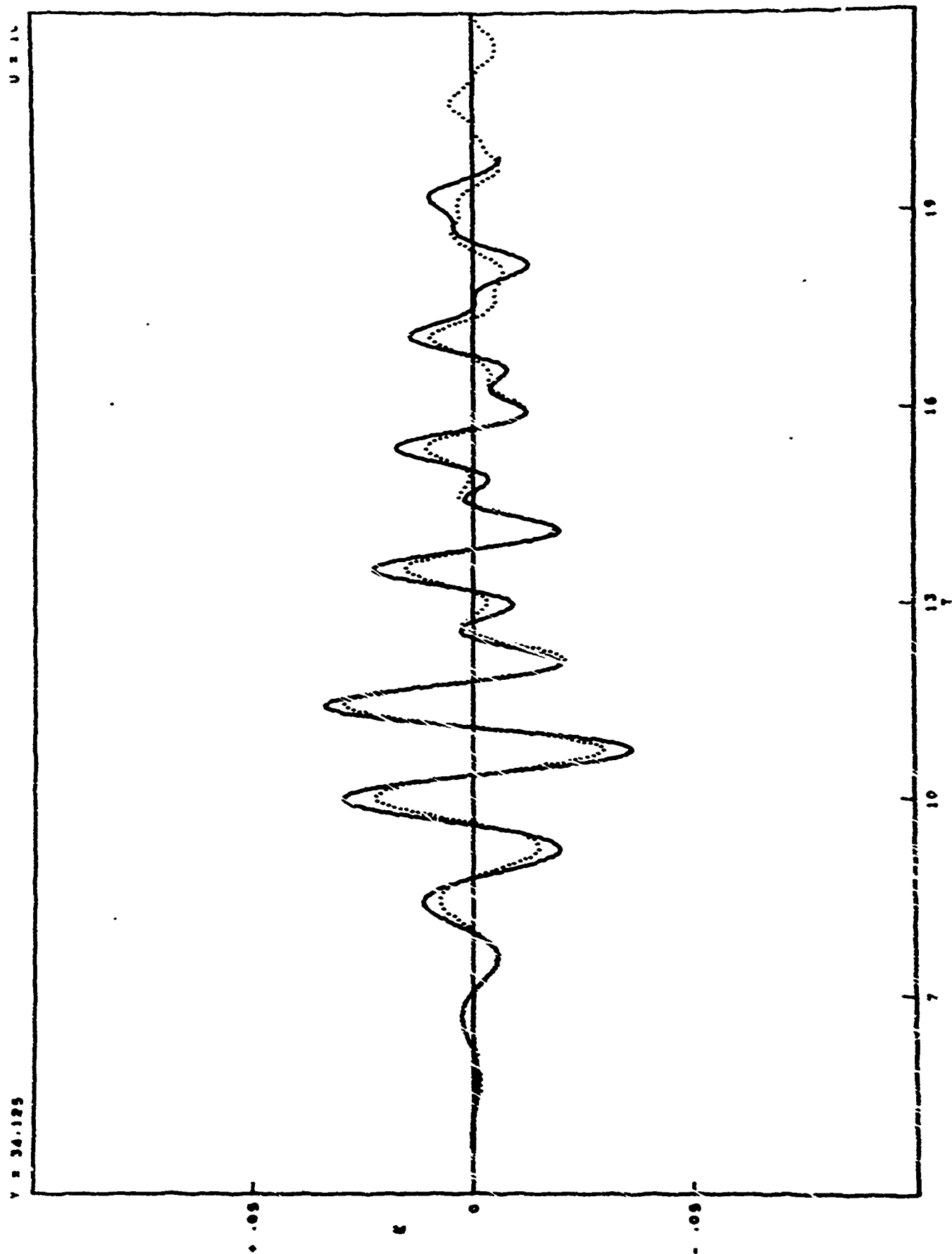


FIGURE 20  
SURFACE ELEVATION



UNCLASSIFIED

Security Classification

## DOCUMENT CONTROL DATA - R &amp; D

(Security classification of title, body of abstract and indexing annotation must be entered when the overall report is classified)

1. ORIGINATING ACTIVITY (Corporate author)		2a. REPORT SECURITY CLASSIFICATION	
Naval Weapons Laboratory		UNCLASSIFIED	
		2b. GROUP	
3. REPORT TITLE			
MEASURED VERSUS COMPUTED SURFACE WAVE TRAINS OF A RANKINE OVOID			
4. DESCRIPTIVE NOTES (Type of report and inclusive dates)			
5. AUTHOR(S) (First name, middle initial, last name)			
Hershey, A. V.			
6. REPORT DATE		7a. TOTAL NO. OF PAGES	7b. NO. OF REFS
7 June 1966		68	
8a. CONTRACT OR GRANT NO.		8b. ORIGINATOR'S REPORT NUMBER(S)	
a. PROJECT NO.		2036	
c.		8b. OTHER REPORT NO(S) (Any other numbers that may be assigned this report)	
d.			
10. DISTRIBUTION STATEMENT			
Distribution of this document is unlimited.			
11. SUPPLEMENTARY NOTES		12. SPONSORING MILITARY ACTIVITY	
13. ABSTRACT			
<p>Measured elevations in the wave train of a Rankine ovoid are compared with computed elevations for an ideal source and sink. The measured elevations are in phase with the computed elevations but have smaller amplitudes. The discrepancy in amplitude is attributed to turbulent boundary layer and wake in the flow around the real ovoid.</p>			

END

DATE

FILMED

12-2-66